



Calcium oxide nanoparticles synthesis from hen eggshells for removal of lead (Pb(II)) from aqueous solution

Reta G. Jalu^a, Tariku A. Chamada^{b,*}, Dr. Ramachandran Kasirajan^c

^a Chemical Engineering Department, School of Chemical Engineering, Wollega University, Nekemte, P.O.Box 395, Oromia, Ethiopia

^b Chemical Engineering Department, School of Mechanical, Chemical and Material Engineering, Adama Science and Technology University, Adama, P.O.Box 1888, Oromia, Ethiopia

^c Chemical Engineering Department, School of Chemical Engineering, Jimma University, Institute of Technology, Jimma, P.O.Box 378, Jimma, Oromia, Ethiopia



ARTICLE INFO

Keywords:

Calcium oxide nanoparticles

Lead

Adsorption isotherms

Adsorption kinetics

ABSTRACT

Lead is an important industrial heavy metal used in various production industries. Remediation of Lead poisoned areas has both economical and technological challenges, as conventional and techniques are very expensive to apply for wastewater treatment and its operation is difficult. The adsorption method could solve the problem using sol-gel-based synthesized adsorbent since it is environmentally friendly with high-quality product produced. In the present study, the application of synthesized calcium oxide nanoparticles from hen eggshells for the removal of lead ions from aqueous solutions is what was investigated. Characterization of the adsorbent like proximate analysis, particle density, bulk density, porosity, point of zero charges, Fourier transform infrared radiation spectroscopy, X-ray diffraction, specific surface area, thermal gravimetric analysis, and scanning electron microscopy was done before batch adsorption experiments. X-ray diffraction revealed that the size of synthesized calcium oxide nanoparticles was 24.34 nm and the specific surface area was 77.4m²/g. The removal of divalent lead ions from aqueous solutions was optimized by using response surface methodology. The optimum percent removal of lead (99.07) has resulted at initial concentration 75.46 ppm, pH 6.94, adsorbent dose 0.838 g, and contact time 101.97 min. The experimental removal efficiency (98.86%) agreed very well with the predicted one (99.07%), showing the suitability of the model used and the success of response surface methodology in optimizing of removal of Pb (II) ions from aqueous solutions. The lead ions removal was well fitted into the Langmuir isotherm model with correlation coefficients of 0.9963. The adsorption kinetic data were well fitted with the pseudo-second-order model with a correlation coefficient of 0.9982. The pseudo-second-order model was the rate-limiting step in the lead (II) ions adsorption process onto CaO NPs. Based on the obtained results, the calcium oxide nanoparticles prepared from eggshell have a good capacity for the removal of the lead ions from the aqueous solutions.

1. Introduction

1.1. Background

The pollution of water resources by industrial effluents containing toxic heavy metal is a matter of great concern because of their non-biodegradable and polluting nature (Afroze and Sen, 2018). Heavy metals have mainly existed in the textile industry, metallurgical operation, acid battery manufacturing, glass industry, and ceramics are the main sources of heavy metal ions that are released into water bodies (Wang, 2012).

Lead is one of the acute between toxic heavy metals (Safatian, 2019). Very low concentrations of lead-heavy metal ions in drinking water

cause diseases like encephalopathy, hepatitis, kidney damage, blood pressure, abortion, improper function in the brain, and the central nervous system of unborn children when it enters a fetus through the placenta of the mother (Woldetsadik, 2017). Environmental legislation obliges industries to eliminate heavy metals from their toxic-containing effluents before disposal into the water. Due to the low-income limit, a lot of industries not successful to provide investment costs in pollution remediation systems and technologies (Amare, 2019). The owners of industries who have enough capital do not interested to fit efficient treatment technologies, because of weak governmental control and weak environmental policy implementations.

The environment can be affected by heavy metal ion pollution. It exists for a long time in soil and water and cannot be decomposed

* Corresponding author at: Department of Chemical Engineering, School of Mechanical, Chemical and Material Engineering, Adama Science and Technology University, Adama, P.O.Box 1888, Oromia, Ethiopia.

E-mail addresses: retagaroma5566@gmail.com (R.G. Jalu), tareefeda2020@gmail.com (T.A. Chamada), ramactech@gmail.com (Dr.R. Kasirajan).

<https://doi.org/10.1016/j.envc.2021.100193>

Received 26 February 2021; Received in revised form 22 June 2021; Accepted 22 June 2021

2667-0100/© 2021 The Author(s). Published by Elsevier B.V. This is an open access article under the CC BY license (<http://creativecommons.org/licenses/by/4.0/>)

AAS	Atomic Absorption Spectroscopy
CV	Coefficient of Variation
CI	Confidence Interval
Df	Degree of freedom
FT-IR	Fourier Transforms Infrared Radiation
ICP-OES	Inductive Coupled-Plasma Optical Emission Spectrometry
IUPAC	International Union Pure Applied Chemistry
JCPDS	Joint Committee on Powder Diffraction Standards
K ₁	Pseudo first-order rate constant
K ₂	Pseudo second-order rate constant
K _f	Freundlich adsorption capacity (mg/g)
K _L	Langmuir equilibrium constant (L/mg)
NAA	Neutral Activation Analysis
NPs	Nanoparticles
PH _{pzc}	Point of zero charge
Ppm	Parts per million
RESP	Raw Eggshell Powder
SEM	Scanning Electron Microscope
TGA	Thermo - Gravimetric Analysis
X-RD	X-Ray Diffraction

like other organic pollutants. Pollutant heavy metal ions are soluble at low pH, and consequently, toxicity problems are relatively higher in the environment. Several treatment methods have been adopted to remove heavy metals from wastewater. Comparatively, adsorption is the most preferred technique due to the simple design, low-cost, and simply operated and can be obtained from locally available materials (Beksissa, 2021). The common adsorbents like activated carbon, silica gel, activated alumina, and ion exchange resins have a good capacity of removing pollutants, but their main disadvantages refer to their high installation and operating cost of treatment and difficult regeneration, which increases the wastewater treatment cost (Crini and Morin-Crini, 2019).

Different forms of biomass can be used for the removal of lead from the point and non-point sources of effluents. A study has been carried out to evaluate the performance of easily available adsorbent for the removal of lead ions from wastewater. Such low-cost adsorbents are promising for commercial use. However, only a few research were done on the sorption studies using eggshell as bio adsorbent. But low removal efficiency on the sorption process, low surface area, and combined effects that occur among process variables were not well addressed (Kaushal, 2017). Waste hen eggshells represent traditionally unwanted substances by the processors and causing unpleasant odors from biodegradation, damaging microbial activity, altering characteristics of the soil (Castro, 2011). The effective uses of waste chicken eggshells are to substitute the commercial of calcium carbonate, calcium hydroxide, and calcium oxide to reduce the waste from the household, conservation of the natural resources like rock, lime, and lime-based materials.

Due to the low-cost and large availability, waste hen eggshells become used in the adsorption process, an attractive and promising technology. Hen eggshell, the main component of pure calcium carbonate (Adeyeye, 2009), is important in the heavy metal ions removal from wastewater but less removal efficiency because of its low porosity. Therefore, synthesizing calcium oxide particles from hen eggshells by sol-gel derived overcomes the shortcomings of the bulk material users because of better performance in terms of higher surface area to its volume ratio, it imparts size-dependent properties such as higher adsorption tendency and large volume wastewater treatment systems.

The benefits of the RSM can be summarised as determining the interaction between the independent variables, model the system mathematically and save time and cost by reducing the amount of testing (Boyaci, 2005).

This study aimed to remove Pb (II) ions from an aqueous solution using calcium oxide nanoparticles as a potential low-cost adsorbent. The effect of operating parameters like pH, contact time, adsorbent dosage, and initial metal ions concentration was studied in a batch adsorption experiment. Adsorption equilibrium isotherm models and adsorption equilibrium kinetic models were carried out during this study.

The comparison of the current method with other recently published work for the removal of Pb (II) has been enumerated in Table 1.

2. Materials and methods

2.1. Materials

Waste hen eggshells were collected from the local area, from restaurants, bakery houses, and chicken poultry places in Jimma city, Ethiopia.

The chemicals used for the study were analytical grade Pb(NO₃)₂ for standard metal ion sample preparation, sodium hydroxide (NaOH), and hydrochloric acid (HCl) were used to adjust the pH value of the solution during the adsorption experiment and shorten the gelation time during CaO nanoparticles synthesis. 1, 5 diphylthiocarbazon (dithizone): This was a photometric reagent that was used to generate colored water-insoluble complexes with a large number of metal ions. H₂SO₄ was used to digest the metal ions in the lead nitrate solution (stock solution). Acetone: was a solvent used to dissolve an aqueous salt suspension for spectrophotometric measurements. Sodium chloride (NaCl): was used as an electrolyte during the determination of the point of zero charges of the adsorbent surfaces. These chemicals and reagents were purchased from a chemical shop in Addis Ababa. Distilled water was used for different experiments in this research. Nitrogen gas was used as an inert atmosphere to avoid oxidation with the sample during thermal treatment as shown in Fig. 1.

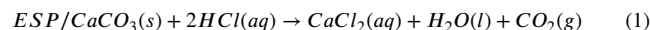
Hen eggshell was the selected source for the preparation of CaO nanoparticles. After collection, the waste hen eggshells were first washed completely with tap water to remove dust, impurities, and organic matters adhered to the surface of the eggshells, followed by another cleaning with distilled water several times. Then the well-washed eggshells were oven-dried at 150°C for 3hr to remove water (Kumaraswamy, 2015). The dried eggshells were ground by a grinder machine to get the fine powder. The fine eggshell powder was passed through a sieve mesh of 100 μm to obtain the finest eggshell powder. The obtained eggshell powder then was kept in a soft polyethylene bag and placed in a sealed plastic container for further study.

2.2. Preparation and characterization of calcium oxide nanoparticles (adsorbent)

Calcium oxide nanoparticles were synthesized from powdered hen eggshell by sol-gel derived technique. Calcium oxide nanoparticles synthesis by sol-gel was obtained at ambient temperature contributing to less energy consumption, with low cost, no additives, a shorter time during preparation, and no pressure. Due to this, it was cheap, green, and sustainable (Lalit, 2019).

Hen eggshell based calcium oxide nanoparticles synthesis with constant reaction parameters were conducted as the following procedures:

- Making a uniform solution of metallic salt, CaCl₂ by dissolving powdered raw eggshell in 36.5% dilute hydrochloric acid. 10.6 g of raw eggshell powder (RESP) was dissolved in 0.25 L of 1 M hydrochloric acid (HCl).

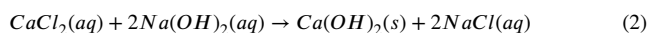


- Development of sol by alkaline hydrolysis reaction. In an aqueous solution, the hydrolysis reaction brings the system more alkaline. Due to this, it had a high ion-exchange capacity. Sol is the liquid state of a colloidal solution made of solid particles, nano-sized in diameter suspended in a liquid phase. By hydrolysis process, metal hydroxide

Table 1
various natural adsorbents for the removal of lead from aqueous solutions.

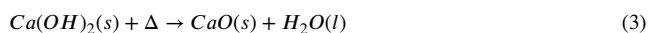
Adsorbent	Optimum pH	Sorbent Dose (g/L)	Concentration (mg/L)	Temperature (°C)	Removal Efficiency (%)	Reference
Fly ash Bagasse	6	10	5–7	30	95–96	(Gupta VK, 2004)
Flash ash modified activated	5	0.5–2	0.558	25	89	(Woolard CD, 2000)
Sawdust activated carbon	5	2	0.1	28	90.1	(Sreejalekshmi KG, 2009)
Activated bamboo	5	0.1	50–90	29	83.01	(Lalhruaitluanga H, 2010)
Peels of banana	5	2	30–80	25	85.3	(Anwar J, 2010)
Coconut	4	6	100	60	60	(Gueu S, 2017)
Coir	4.9	1	0.12	30	86.98	(Shukla SR, 2005)
Shells of hazelnut	7	0.1	0.207	25	90	(Pehlivan E, 2009)
Onion skin	6	0.15	25–200	30	93	(SakaC, 2011)
Ash of rice husk	5	5	3–100	30	89.3	(Nuiya TK, 2009)
Tea waste	5	0.5	5–100	30	96	(Ahluwalia SS, 2005)

(M-OH) was formed. 1 M in 250 mL, of caustic soda (99%) concentration was added drop by drop to change the solution of sodium chloride generated in Eq. (1) above into sol at room temperature. The gradual addition of aqueous caustic soda to the solution was to give precipitation of calcium hydroxide one over another generating a highly crystalline gel.



The gel was generated by a condensation reaction. The condensation reaction occurred when two molecules join to form a larger molecule and release a smaller molecule in the process. Here the smaller molecules lost in the reaction was solution sodium chloride. Calcium hydroxide, gel- containing solution stayed for 24 hrs at ambient temperature to condense very well. Filtration was the next activity after condensation with the help of centrifuge at 3000 rpm to obtain Ca (OH)₂ gel. The filtered Ca(OH)₂ was washed with distilled water to get rid of impurities from the precipitate (Zahra Mirghiasi, 2014).

- Finally, water was removed from the generated precipitate by drying at 60 °C for one day in the heating oven. And lastly, calcined the dried powder at 900 °C for 1 hr using a muffle furnace (Rohim, 2014).



Eggshell samples were characterized by proximate analysis, Fourier-transform infrared spectroscopy (FT-IR), X-ray diffraction (XRD), Thermo-gravimetric analysis (TGA), Scanning Electron microscope (SEM), and Specific Surface Area.

i Proximate analysis

Proximate analysis is one of the thermal analytical techniques in which physical property is measured with a temperature-programmed difference. The one physical property measured was the mass (weight). A hen eggshell/CaO sample as an adsorbent, the physicochemical characteristics like moisture content, ash content, volatile matter, and fixed carbon were determined by adding 8 gm of samples in the crucible and keeping them in a hot air oven and muffle furnace respectively at a different temperature and time. The weights of both samples were recorded before and after drying.

2.3. Preparation of adsorbate

The wastewater contains different pollutants such as dyes, different organic compounds, soluble and insoluble substances, and other metal ions. So it was very difficult to control at the laboratory to treat or to separate these all pollutants. In this case, studying the effect of lead (Pb²⁺) metal ion onto nano CaO alone was appropriate. To avoid the disturbances of other soluble substances that occurred in regular tap or drinking water, distilled water was used to dissolve the metal crystals.

Lead nitrate was helping as the source of the lead stock solution. All necessary solutions have been prepared with analytic reagents and de-ionized water. Pb (NO₃)₂ was used to give a clear colorless lead solution. A lead stock solution with (1000 mg/L) was prepared by dissolving

1.6146 g of 99% Pb(NO₃)₂ within 1 L of distilled water to prepare synthetic Pb (II) ions solution as a model pollutant and this was also used to prepare the working solutions with different initial lead concentrations by taking different dilution amounts.

2.4. Experimental set-up and design

2.4.1. Batch adsorption experiment studies and experimental set-up

Batch adsorption experiments were set for performing all experiments. All experiments were conducted in a conical flask of 250 mL capacity. In each experiment, the solution volume was 100 mL. The mixture of solution and the adsorbent were agitated by using a magnetic stirrer on a hot plate at 250 rpm. Initial solution pH was adjusted using a pH meter by dropping 0.1 M HCl or 0.1 M NaOH before adding the adsorbent to the solution. The temperature of the process was adjusted ambient on a hot plate and initial Pb (II) ion concentration was taken from synthetic Pb (II) ion solution by measuring cylinder. After batch adsorption was completed, the samples were filtered with the help of What-man filter papers, and the liquid lie above the solid residue was analyzed for Pb (II) ion by UVvisible spectrophotometer Fig. 9.

The amount of contaminant adsorbed onto the unit weight of the adsorbent at equilibrium and at any time t were calculated based on mass balance equations given by the following equations, (Ghaneian, 2017):

$$q_e = \frac{V(C_o - C_e)}{m} \quad (4)$$

$$q_t = \frac{V(C_o - C_t)}{m} \quad (5)$$

Where q_e and q_t are, the amounts adsorbed (mg/g) at the equilibrium and at any time t, respectively.

C_o , C_e and C_t are the concentration of the Pb (II) in the solution (mg/L) at the initial, equilibrium, and at time t, respectively; V is the volume of the solution (L), and m is the mass of the adsorbent (g).

The removal efficiency (E) of the adsorbent can be calculated as (Ghaneian, 2017):

$$\%Removal = \frac{100(C_o - C_t)}{C_o} \quad (6)$$

Where C_o and C_t (mg/L) are the initial and final concentration at time t of the Pb (II) in the solution, respectively.

2.5. The effect of pH, adsorbent dosage, contact time, and initial concentration on the adsorption of Pb (II)

2.5.1. pH

The effect of the solution pH on lead metal ions removal using calcium oxide particles used as a selective adsorbent was carried out; using a 100 mL solution of 60 mg/L of metal ion solution in the pH range of one to eleven with two pH interval at ambient temperature and adsorbent dosage used was 0.75 g/100 mL solution. Flasks were shaken on a shaker for 250 rpm shaking speed and 105 min contact time to



Fig. 1. Synthesis steps of CaO NP adsorbent A) Raw hen eggshells B) Washed hen eggshells C) Oven-dried eggshells D) sieved eggshells after ground E) preparation of homogeneous solutions F) Hydrolyses reaction G) condensation reaction H) Gel- filtration process I) Oven drying of Collection of filtered gels J) Muffle furnace calcination of dried gels K) Cancinated Gel powders (CaO NPs).

make sure equilibrium is attained. After equilibrium was attained, the solutions were filtered and analyzed to determine the lead metal ion concentration.

2.5.2. Contact time

The effect of contact time for the removal efficiency and maximum contact time for the adsorption process was studied by experimenting with 15 to 135 minutes with a 15minute time interval staying the other parameters like pH, initial concentration, and adsorbent dose all constant at 7, 60 mg/L, and 0.75 g respectively. The experiment was car-

ried out at a 250 rpm shaker at ambient temperature. As soon as the time required for adsorption arrived the adsorbent (residuals) and the solution was filtered by what man 0.45 filter paper. The filtered solution was analyzed using UV-spectrophotometer for the remaining lead in the solution concentration.

2.5.3. Adsorbent dosage

The effect of adsorbent dosage was studied by experimenting with 0.25 to 1.5 g/100 mL of CaO particle with 0.25 g the difference while staying the other parameters such as initial concentration, pH, and con-

tact time remain constant at 60 mg/L, 7, and 105 minutes respectively. The experiments were carried out at room temperature and 250 rpm shaker speed. After the adsorption was completed the solution and adsorbent were filtered. The filtered solution was analyzed using UV-spectrophotometer to know the remaining lead solution, and then followed estimation of removal efficiency plot versus adsorbent dose used.

2.5.4. Initial concentration of Pb (II)

The most relevant factor in the Pb (II) adsorption process was the initial concentration. The sample in the concentration range of 30–150 mg/L with 30 mg/L interval was prepared for determining the influence of the initial concentration of lead on the removal efficiency. Then it was put on the shaker at speed of 250 rpm and room temperature by maintaining the pH, adsorbent dose, and residence time, all remains constant at 7, 0.75 gm, and 105 min.

2.6. Adsorption kinetics study

Adsorption kinetics study could give grasping of the adsorption rate and controlling their adsorption mechanism. These experiments were carried out by varying the contact time from 15 to 135 min at ambient temperature, staying other parameters remain constant such as pH, adsorbent dose, and initial metal ion concentration at 7, 0.75 g, and 60 mg/L respectively. The samples were shaken at speed of 250 rpm and withdrawn at a 15minute time interval to determine the residual of lead ion in the solution. Then data from the experiment was provided into the pseudo-first-order model, pseudo-second-order, and intra-particle diffusion (Dagmawi, 2013).

2.7. Adsorption isotherm models

Adsorption isotherms were used to study the relationship between the quantity of Pb (II) ion adsorbed onto the CaO NPs surface and the concentration of a lead ion in the aqueous phase at equilibrium. On the equilibrium, equal amounts of solutes are adsorbed and fluid desorbed at the same time. This is termed adsorption equilibrium. The relationship between the amount of substance adsorbed per unit mass of adsorbent at constant temperature and its concentration in the equilibrium solution is termed as adsorption isotherm. Adsorption isotherm models like Langmuir, Freundlich, and Temkin, models were used for fitting the experimental data. It is used to find the best fitting isothermal model to calculate the efficiency of the synthesized adsorbent and to advance the appropriate batch adsorber design. The adsorption capacity at equilibrium, q_e (mg/g) was calculated by the Eq. (4) above.

The Langmuir equations of non-linear and linear expressions are given in Eqs. (7) and (8).

$$q_e = \frac{q_{\max} k_L c_e}{1 + k_L c_e} \quad (7)$$

Where q_e is the quantity of metal ions adsorbed per gram of adsorbent at equilibrium, q_{\max} is the maximum quantity of the metal ion per unit weight of the adsorbent to form a complete monolayer on the surface-bound at high C_e , where C_e is the concentration of metal ions in solution at equilibrium and K_L is a Langmuir constant. The linear form of Langmuir isotherm is (Jonas Bayuo, 2019):

$$\frac{c_e}{q_e} = \frac{c_e}{q_{\max}} + \frac{1}{K_L q_{\max}} \quad (8)$$

Where q_{\max} and K_L are computed from slope and intercept of Langmuir plot of C_e/q_e against C_e with a slope of $\frac{C_e}{q_{\max}}$ and intercept of $\frac{1}{q_{\max} K_L}$. The fitness of adsorption to Langmuir isotherm process model can be expressed in terms of the equilibrium parameter R_L , which is the dimensionless constant and can be expressed as:

$$R_L = \frac{1}{1 + K_L C_0} \quad (9)$$

Where C_0 is the initial metal ion concentration and R_L is the separation factor and the value shows the adsorption nature to be unfavorable when $R_L > 1$, linear when $R_L = 1$, favorable when $0 < R_L < 1$, and irreversible when $R_L = 0$.

Freundlich isotherm depicts that the measure of the quantity of solute adsorbed onto a given solid adsorbent to the concentration of solute in the solution is not remain constant at different concentrations. This model takes the following exponential equation for single-component adsorption (Sanjay, 2014).

$$q_e = K_f C_e^{1/n} \quad (10)$$

Where C_e is the liquid phase sorbent concentration at equilibrium (mg/L), q_e is the solid phase equation is: concentration at equilibrium (mg/g), K_f is the Freundlich constants and $1/n$ is the heterogeneity factor. K_f and $1/n$ are indicators of adsorption capacity and adsorption intensity respectively. The linearized form of the above.

If the value of n ranges from 2–10, it represents good, when it ranges between 1–2, it represents moderately good, and if less than 1 poor adsorption characteristics (Igwé, 2007).

This kind of adsorption isothermal model is based on the assumption that the heat of molecules decreases linearly with an increase in coverage of the adsorbent surface (Ringot, 2007).

This model is expressed as:

$$q_e = \frac{RT}{b} \ln(ACe) \quad (12)$$

The linearized form of the Temkin equation is expressed as follows:

$$q_e = \frac{RT}{b} \ln A + \frac{RT}{b} \ln C_e \quad (13)$$

$$q_e = B \ln K_T + B \ln C_e \quad (14)$$

Where R is gas an ideal gas constant (8.314 J/mol/K), T is the temperature (K), q_e is the amount of lead adsorbed at equilibrium, C_e equilibrium concentration in mg/L, A is Temkin isotherm constant (L/g) and b is the heat of sorption (J/mol).

The pseudo-first-order model which is believed to be the earliest model and was developed by the Lagragren equation (Ho,1999). The first-order model kinetics of liquid-solid phase adsorption can be described as follows:

$$\frac{dq_t}{dt} = K_1(q_e - q_t) \quad (15)$$

Where, the q_e and q_t (mg/g) are the adsorption capacity at equilibrium and time, t (min), respectively.

K_1 (min^{-1}) is the pseudo-first-order rate constant for the kinetic model. Integration of the equation with the boundary conditions $q_t=0$ at $t=0$ and $q_t=q_t$ at $t=t$, yields

$$\ln \left(\frac{q_e}{q_e - q_t} \right) = K_1 t \quad (16)$$

The linearized form of the equation above is expressed in the form of:

$$\log(q_e - q_t) = \log q_e - \frac{k_1 t}{2.303} \quad (17)$$

The equilibrium adsorption capacity q_e and the pseudo-first-order constant (k_1) can be evaluated experimentally from the slope ($\frac{-k_1}{2.303}$) and intercept $\log(q_e)$ of plotting of $\log(q_e - q_t)$ versus t respectively.

The adsorption kinetics data of the second-order model can be expressed as:

$$\frac{dq_t}{dt} = k_2(q_e - q_t)^2 \quad (18)$$

Integrating the equation for the boundary conditions $t = 0$ to $t = t$ and $q_t=0$ to $q_t=q_t$, brings:

$$\frac{1}{q_e - q_t} = \frac{1}{q_e} + K_2 t \quad (19)$$

Table 2
Design experimental factors and levels used in CCD.

Independent parameters	Coded factors	Coded levels				
		$-\alpha$	-1	0	+1	$+\alpha$
Metal initial concentration (mg/L)	A	30	60	90	120	150
pH	B	1	3	5	9	11
Adsorbent dose (g)	C	0.25	0.5	0.75	1	1.25
Contact time (min)	D	15	45	75	105	135

This can be linearized as follows:

$$\frac{t}{q_e} = \frac{1}{q_e^2 k_2} + \frac{1}{q_e} t \quad (20)$$

q_e is the amount of lead adsorbed at equilibrium (mg/g) and k_2 is the equilibrium rate constant of the pseudo-second-order sorption, (g /mg.min). The constants, q_e , and K_2 are obtained from the slope $\frac{1}{q_e}$ and intercept ($\frac{1}{k_2 q_e^2}$) of t/q_t versus t linear plot, respectively.

When intra-particle diffusion participates in the adsorption process, the plot of the square root of time (i.e. \sqrt{t}) against uptake q_t would bring a linear relationship and would be also a controlling step if the line pass via the origin (Latif, 2010). An equation for this model can be written as:

$$q_t = k_t t^{0.5} + C \quad (21)$$

Where q_t is the amount of metal adsorbed at a time (mg/g), K_t is the intra-particle diffusion rate constants (mg/g.min^{0.5}) and, C is the intercept and constant. The intra-particle diffusion rate constant (K_t) is obtained from the slope and the intercept of the linear plot of q_t versus ($t^{0.5}$) at different initial metal concentrations and ambient temperature.

2.8. Experimental design

2.8.1. Central composite design (CCD)

The Central Composite Design (CCD) was used for the optimization of lead adsorption onto CaO particles by applying Response Surface Methodology (RSM) with five levels as shown in Table 2. It was used to investigate the effects of four factors namely, initial Pb (II) ion concentration (A), pH (B), contact time (C), and adsorbent dosage (D) on the response, percentage of Pb (II) ion removal (Y). RSM was used to evaluate the effect of the individual factors, the interaction effects of the variables, and the optimum condition of the responses. The experiments were carried out and data were statistically analyzed by the design-Expert (Stat-Ease, Inc., version 11.1.0.1,) to find the suitable model for the percentage of Pb (II) ion removal yield as a function of the above four factors. Design expert software version 11.1.0.1 was applied for the ANOVA and the optimization of process parameters for adsorption. The central composite design was used to reduce the number of experiments and increase the interaction effect among all factors. From the central composite design we can use the formula:

$$N = 2^K + 2K + n_0 \quad (22)$$

Where N stands for the number of experiments, k is the number of factors and n_0 is the number of the replications. Therefore in this research, the number of experiments required were, $N=2^4+2*4+6=30$

Based on the works of literature the selected ranges of the factors were pH between 3 to 7, the dose from 0.5 g to 1 g, and the initial metal concentration between 60 mg/L and 120 mg/L, and contact time 45 min to 105 min.

2.8.2. Development of regression models equations

The Response surface methodology gave the empirical relationship between the response function and the independent variables (factors). The quadratic response model was based on all linear terms, quadratic

Table 3
Summary of proximate analysis results.

Parameter	Value in %	
	Raw eggshells	CaO particles Adsorbent
Moisture Content	0.98	0.135
Ash Content	78.2	99.06
Volatile Matter	2.7	—
Fixed Carbon	18.12	—

terms, and linear interaction terms according to the following equation (Jonas, 2019) given by Eq. (8):

$$Y = \beta_0 + \sum_{i=1}^k \beta_i X_i + \sum_{i=1}^k \beta_{ii} X_i^2 + \sum_{i < j} \beta_{ij} X_i X_j \quad (23)$$

Where: Y= predicted response, β_0 = constant-coefficient, β_i = linear coefficients, β_{ii} = quadratic coefficients, β_{ij} = interaction coefficients, X_i and X_j were coded values for the factors.

3. Results and discussions

3.1. Evaluation of proximate analysis of raw eggshell and CaO particles

Proximate analysis was performed for both raw eggshell and CaO particles adsorbent to analyze the different physicochemical characteristics such as moisture content, ash content, volatile matter, and fixed carbon was shown in Table 3.

The moisture content of both raw eggshells and CaO Particles adsorbents was found to be 0.98 and 0.135 percentage respectively. The purpose of measuring the adsorbent moisture content was to identify the adsorbent's better removal capability. The sample's moisture content tells us the percentage of water capacity present in the sample. The percentage of moisture content of both raw eggshell and CaO Particles which were somewhat lower than the value reported elsewhere in the literature, 1.174% (Bhaumik et al, 2012; Woldemedhin, 2021). However, from the result above CaO NPs had very stable with good quality and longer shelf life than the RESP. The smaller the percentage of moisture content, the maxima of its adsorption efficiency, as a result, the presence of water in the adsorbent can occupy the adsorbent active sites before it contacts with the solution. Therefore, the adsorption percentage decreased with an increase in the moisture content of the adsorbent (Getasew Ketsela, 2020).

The ash content is a reflection of the amount of inorganic substituent present in the eggshell and CaO was obtained as 78.2% and 99.06% respectively. This percentage was larger than the ash content of hen eggshell recorded in the former literature 45.29% (Ajala, 2018). The higher the ash content values, the higher the quality of the adsorbent for higher removal efficiencies (Getasew Ketsela, 2020).

Volatile matter is due to the residual organic compounds in the prepared adsorbent and the value of volatile matter obtained in powdered hen eggshell was 2.7%. Since this value is very small, it has no influence on the adsorbent generated after calcination of calcium hydroxide, gel from hen eggshells.

Fixed carbon is the combustible solid residue left after calcium hydroxide from hen eggshell was heated and the volatile matter was dismissed. The content of fixed carbon in hen eggshell was calculated by summing the percentage of moisture content, ash content, and volatile matter and subtracting from total samples. Then the value calculated was 18.12%.

Laboratory results of particle densities for both RESP and CaO nanoparticles were 0.98 g/cm³ and 2.01 g/cm³ respectively. These results showed us that the particle density of calcium oxide nanoparticles was greater than that of the raw eggshell powders. The larger the particle density the higher porosity of the adsorbent has resulted.

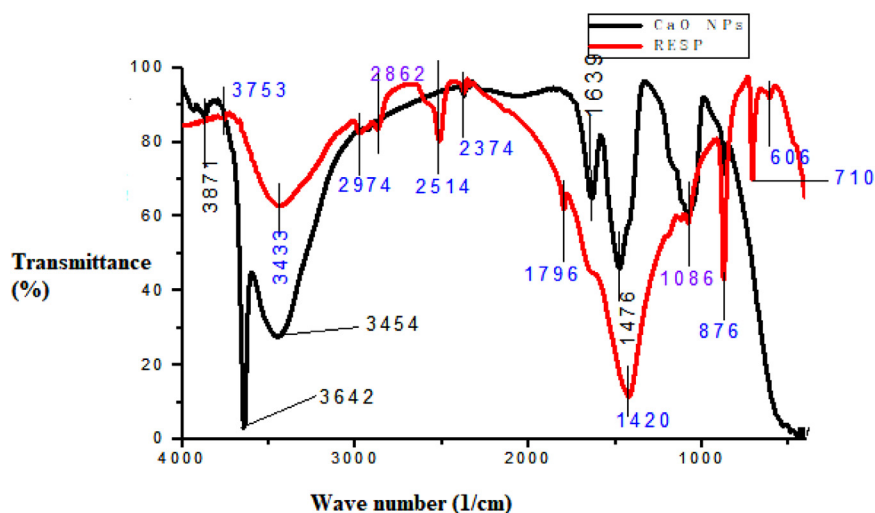


Fig. 2. FT-IR for CaO NPs and RES Powders.

The RESP and calcium oxide nanoparticles' bulk densities were 0.719 g/cm^3 and 0.375 g/cm^3 respectively. These values were less than the bulk density of hen eggshell reported somewhere in the literature 2.20 g/cm^3 (Tangboriboon, 2012). From these results, the bulk density of raw eggshell was greater than that of calcium oxide nanoparticles. The greater the bulk density the lower porosity of adsorbent has resulted. From those adsorbent studies, the particle density increases from RESP to CaO NPs whereas the bulk density decreased from RESP to CaO NPs and this shows the porosity is low with a high value of bulk density and high with a high value of particle density.

From the above particle density and bulk density calculations, the porosity of RESP and CaO NPs were 26.63% and 81.34% respectively. From the research carried out on biomasses, there are linear relationships between porosity and adsorptive processes (Malik, 2006). The higher the porosity of an adsorbent it had the relatively larger potential for adsorbing the adsorbate. Therefore synthesized calcium oxide nanoparticles from hen eggshell had higher porosity than its bulk materials.

3.2. FT-IR spectra of analysis of RESP and CaO NPs derived from hen eggshell

FT-IR analyses were carried out to understand the possible interactions between biological molecules and lead ions during the reduction reaction. The FTIR spectrum of RESP and CaO nanoparticles were tested to get information about the bending and stretching vibrations of the functional groups. Fig. 2 depicts the FT-IR analyses for RESP and CaO NPs synthesized from hen eggshell traveling across numerous bands from $4000\text{--}400 \text{ cm}^{-1}$. From the figure of RESP, the bands, 876 cm^{-1} , 1420 cm^{-1} , and 2514 cm^{-1} represent the G-O stretching and bending of the CaCO_3 , the main component of the RESP, bands 3433 cm^{-1} stand for H_2O , bands 2862 cm^{-1} and 1796 cm^{-1} stand for C=O. The sharp band at 710 cm^{-1} represents a Ca-O bond.

As depicted from Fig. 3, both RESP and CaO NPs spectra of carbonate, CO_3^{2-} occurs at 876 cm^{-1} . The existence of this band revealed the oxygen atom of the carbonate and calcium in the raw eggshell. The sharper band of CaO NPs at 1476 cm^{-1} and 876 cm^{-1} in the figure below shows that the stretching of the G-H bond indicating the carbonization of CaO NPs. The adsorption peaks at 3642 cm^{-1} and 3454 have resulted because of the O-H bond from water molecules (moisture) on the surface of CaO NPs (Zahra mirghiasi, 2014). The absence of a sharp band (606 cm^{-1}) in the spectra of RESP indicates that the calcium carbonate, the main component of hen eggshell was no longer present; it was already converted to calcium oxide nanoparticles. Almost the uniformity of peaks for all RESP, CaO NPs, and lead loaded CaO NPs after the ad-

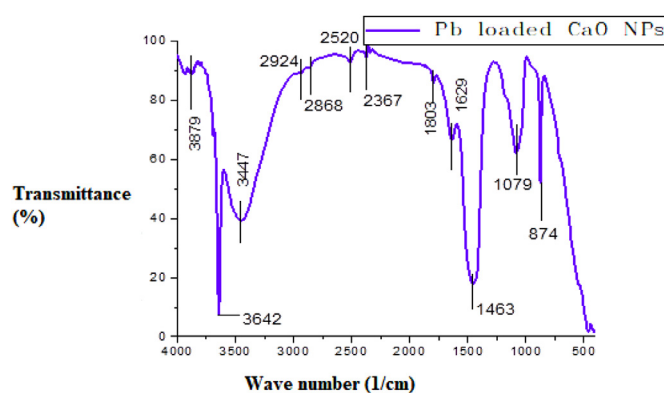


Fig. 3. FT-IR for lead loaded CaO NPs.

sorption experiment was due to the absorbance of moisture and carbon dioxide from the environment. The FT-IR spectrum of the CaO NPs exposed to Pb (II) ions showed a decrease in the intensity of the peaks and some shifts or changes in the wavenumbers. Table 4 below depicts the main difference between the wavenumbers before and after Pb (II) adsorption process. The changes in the wavenumbers were small, less than 15 cm^{-1} . This result indicated the possibility that the adsorption process could be taken place via an ion-exchange process or physical interaction (Blázquez, 2010).

3.3. X-ray diffraction (XRD) structure analysis of CaO NPs and RESP

To establish the truth whether the synthesized sample was CaO NPs or not and to investigate the structure of nanoparticles, XRD analysis was behaved and showed good agreement with the Joint Crystal Powder Diffraction Standard (JCPDS) card number 77-2376.

The peaks were observed at $2\theta=32.48, 37.45, 54.012, 64.22, 67.63, \text{ and } 88.68$ that were allocated with (111),(200),(220),(311), (222),(400), and (331) plane phase of CaO respectively. The principal peak has appeared at $2\theta=37.45$ and the sharp peaks and narrower spectral width in the XRD pattern revealed good polycrystalline nature of CaO NPs. The result demonstrated that the larger composition in hen eggshell (calcium carbonate) was thoroughly converted to calcium oxide during synthesis; because the XRD result has no any peak formed at $2\theta=29.55$ as the peak in the RESP, it was completely changed to CaO NPs. None of the peaks corresponding to impurities were found; showing that high-quality CaO was generated.

Table 4
FT-IR spectral characteristics of CaO NPs before and after Pb (II) ion adsorption.

Functional groups Of IR adsorption bands	Wavenumber, cm-1 Adsorption Bands		
	Before adsorption of Pb(II) ion	After adsorption of Pb(II) ion	Shift difference
OH, hydroxyl	3454	3447	7
C = C, Alkenes	1639	1629	10
G- C=C, symmetric	1476	1463	13
C = O, carbonyl	876	874	2
G- N,carboxylic acid	1086	1079	7

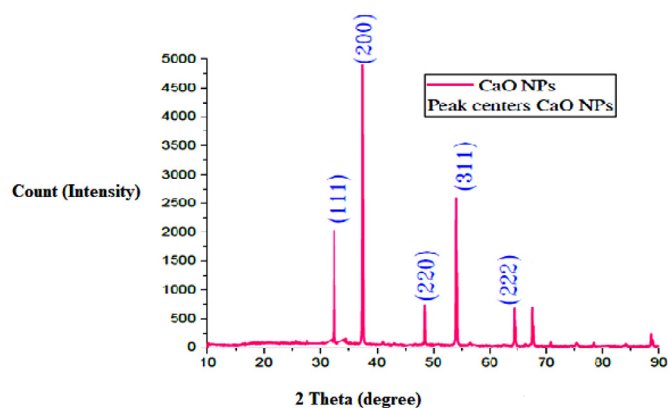


Fig. 4. XRD plot of synthesized Calcium oxide nanoparticles.

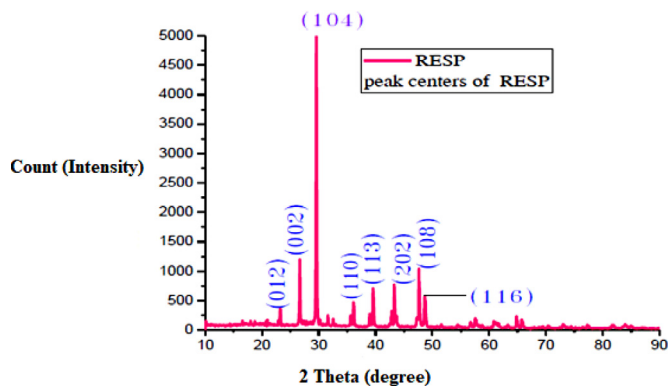


Fig. 5. XRD plot of raw eggshell powder.

Spherical geometry of calcium oxide has resulted during the synthesis of calcium oxide nanoparticles after calcination. The average crystallite size was calculated by the debye-Scherrer formula and found to be 24.34 nm for the crystallographic of CaO which confirmed that the synthesized nanoparticles were nanocrystalline in nature. A similar result was obtained by (Ashok, 2015).

Fig. 4 shows the qualitative phase study of the un-calcined raw eggshell. The analysis for un-calcined eggshell powder revealed the existence of the CaCO_3 phase as major components of the sample. All the characteristics peaks observed from Fig. 5 were fitted with the calcium carbonate phase (JCPDS Card No. 00-081-2027). The main peak appeared at $2\theta=29.55$. The other peaks with their respective planes: 23.2, 26.76, 29.55, 36.06, 39.62, 43.17, 47.66, 48.59 and (012), (002), (104), (110), (113), (202), (018), (116) respectively.

Using the scherrer equation the average size of the crystallite was 79.4 μm . Through the analysis hexagonal structure was obtained in this work. A similar result was obtained.

3.4. Thermogravimetric analysis of RESP, calcium hydroxide, and CaO NPs

It is used to measure the mass change of a sample as a function of temperature or time, under a defined and controlled environment with respect to heating rate, gas atmosphere, flow rate, crucible type, etc.

The raw eggshell powder decomposition temperature was obtained from the TGA curve. The thermogravimetric analysis (TGA) of RESP was conducted between ambient temperature and 1000°C to determine thermal stability and decomposition temperature. The TGA result showed that significant weight loss was appeared between the temperature of around 600 and 850°C because of removed impurities and the raw eggshell powder residue was stable above 850°C as shown from Fig. 12, because CO_2 was released to the environment. In a raw eggshell, a total weight loss of 45.62% was noticed. The mass loss was related to the loss of volatile substances like water and organic materials. In the second region, the mass loss was due to the release of CO_2 from CaCO_3 decomposition.

The first weight-loss stage was due to the vaporization of the adsorbed water with a weight loss of 45.701%, between temperatures of 45.14°C-432.05°C.

The second stage was due to the decomposition of gel ($\text{Ca}(\text{OH})_2$) to CaO, with mass loss of 31.1%, between temperatures of 432.05°C-631.32°C and the end-stage was due to the breakdown of CaCO_3 into CaO and release of carbon dioxide, with mass loss of 3.6%, between the temperatures of 631.32°C-865.6°C. The gel was stable or has no significant weight loss above 865.6°C, and the total weight loss obtained up to a temperature of 865.6°C was 80.4%.

The CaO NPs adsorbent had only a slight weight loss of 4.7% between the temperatures of 356 to 385 °C. This amount of weight loss was observed due to the loss of CO_2 during the carbonization of CaO NPs had high thermal stability and purity as shown in Fig. 14.

As observed from the TGA curves, the decomposition temperatures of the raw eggshell powder and $\text{Ca}(\text{OH})_2$ gel was 850°C and 865.6°C respectively. No mass loss was noticed after these respective temperatures. This revealed that the heating temperatures of not lower than these values are required for thermal decomposition of the two respective samples as shown in Fig. 13.

3.5. Scanning electron microscopy (SEM)

The morphology and texture of CaO NPs were studied by using SEM. It revealed that the NPs were spongy-like and foamy products with large agglomerates of very small particles. The surface morphology of the adsorbent particles through investigating the picture/image shows that the synthesized size particles were a lesser size and therefore the adsorbent/sorbent has increased surface porosity with 10 μm magnifications. As observed from the image CaO particles had regular morphology with a uniform size. This indicates that the sol-gel process can make the crystal structure of CaO more orderly Fig. 10.

The bright parts of surfaces from the image reveal high emission of electrons when exposed to the electron beam of SEM. This showed the high surface area to volume ratio in the bright parts of surfaces. As it was observed from the micrograph, the synthesized particles were made of grains with spherical shapes agglomerated to each other. These small

particles agglomerated to each other reveal the polycrystalline character of CaO NPs. Other investigations confirmed the spherical shape of CaO NPs (Zahra margins, 2014). Also as shown from the image, the crystal structures of CaO particles were interconnected skeletal rather than irregular due to the calcination process. The porosity of CaO particles was due to the release of CO_2 and H_2O from the internal structure, during the calcination of $\text{Ca}(\text{OH})_2$. The existence of the developed pores in the CaO microspheres facilitates efficient removal activity of heavy metal from wastewater. Easy separation of heavy metals from wastewater was due to the high surface area, uniformity, and porosity of CaO NPs.

3.6. Point of zero charge (PHpzc) analysis

Point of zero charges was formulated by acid/base titrations of a colloidal dispersion of CaO particles in the salt solution. It was crucial to find the point of zero charges (pHPzc) of the adsorbent to investigate the surface behavior of the adsorbent and the influence of pH in the adsorption process. When $\text{pH} < \text{pHPzc}$, the surface charge on the adsorbent is a net positive charge, and when $\text{pH} > \text{pHPzc}$, the surface charge on the adsorbent is a net negative charge. Therefore, anions adsorption on the surface of the adsorbent is favorable at a pH value lower than pHPzc and cations adsorption on the adsorbent surface is favorable at a pH value higher than pHPzc. From the analysis the point of zero charges obtained from the experimental results was pH 6.82 this was greater than pH 6.3 which was reported in the literature (R.Bhaumik, 2012).

The CaO NPs adsorbents work best at the cationic molecule of acidic surface charge. Therefore this indicates that cations adsorption was enhanced at $6.82 < \text{pH}$, hence a pH of greater than 6.82 ($\text{pH} > 6.82$) was preferable for cationic adsorptions. Therefore, the adsorption of the Pb (II) was favored at pH greater than the pH_{pzc} where the surface of the adsorbent becomes negatively charged as shown in Fig. 11.

The pH value kept greater than the obtained pHPzc, 6.82 to make a powerful negatively charged surface which causes electrostatic attraction between the molecule of adsorbate and adsorbents. Less than this pH, the surface charge of the adsorbent gets positively charged because of the protonation of functional groups which making H^+ ions that compete well with Pb cations, these results in a decrease in the expected amount of adsorbate adsorbed on vacant active sites. In general, adsorption of the cations increased with increasing pH, whereas adsorption of anions increases with decreasing pH.

3.7. Determination of specific surface area

As described under material and method, the determination of surface area was calculated. The titrated volume using NaOH to raise the pH of the solution from four to nine were 1.95 and 3.2 mL of RESP and CaO NPs respectively. Substituting these numerical values in the above equations, the specific surface area of RESP was $37.4 \text{ m}^2/\text{g}$, this was greater than $21 \text{ m}^2/\text{g}$ (Viriyempikul, 2012). The CaO NPs surface area was $77.4 \text{ m}^2/\text{g}$. These values lay between 60 and $90 \text{ m}^2/\text{g}$ of the specific surface area reported by (Ohmi, 2009). From this titration experiment synthesizing nanoparticles adsorbent and calcination process increases the specific surface area of the adsorbents. In general, the larger the specific surface area of the adsorbent, the better is the adsorption performance.

3.8. Pb (II) adsorption studies

At the end of the lead adsorption study, the residual/suspension was separated through filtration processes. After filtration; the lead concentrations were determined by UV-spectrophotometer, from the calibration curve. All 30 run experiments were done with a different combination of four parameters and the values were recorded as illustrated in the Appendix G.

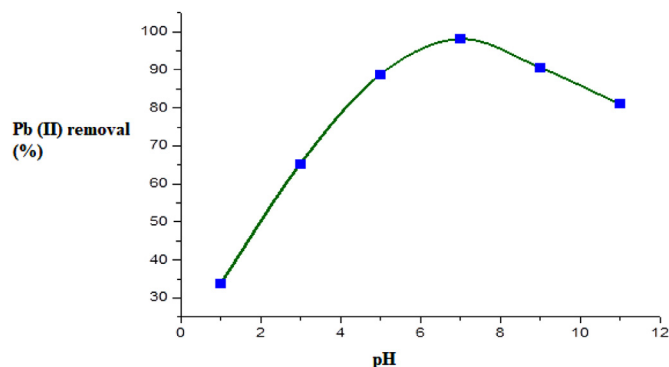


Fig. 6. Effect of pH on Pb (II) removal.

The investigation adsorption process of Pb (II) on calcium oxide nano-particles characterizations have been discussed considering the effect of individual factors.

3.8.1. Effect of pH on Pb (II) removal

The adsorption of lead (II) ions from an aqueous solution using CaO nanoparticles applied in this research was highly dependent on the pH of the solution. The dependency of metal uptake on pH is related to both the ionization state of the functional groups on sorbent and the metal chemistry of the solution. The graph illustrated in Fig. 6 indicated that the removal percentage of Pb (II) ions increased with increased pH. This was because the point of zero charges of the calcium oxide nanoparticles was at 6.82. The positively ionic adsorption process is preferred at a pH greater than the pH point of zero charges. Lower Pb (II) removal efficiency was 33.83% at pH 1 and higher Pb (II) removal efficiency was 98.12% at pH 7. At lower pH, H_3O^+ ions compete against Pb (II) ions for binding to the adsorbent and encircled hydronium ions (H^+) discontinuation metal ions from approaching the binding sites and it leads to low adsorption capacities. Positively charged metal ions and positively charged sites were powerless of binding metal ions due to electrostatic repulsion. Because of this, a low removal percentage of Pb (II) was observed. There existed fewer H^+ ions take place in the solution when pH increased and as a result more negatively charged sites were made and higher metal ion removal was achieved by electrostatic attraction. In alkaline conditions of pH greater than 7, the removal efficiency was reduced. This was because at low pH (< 7), positively charged Pb (II) species are dominant and adsorption on CaO NPs takes place at a faster rate. But in the case of pH values ($\text{pH} > 7$), the adsorption was reduced due to different production of lead species with different charges like $\text{Pb}(\text{OH})^+$, and $\text{Pb}(\text{OH})_2$ (Gupta VK, 2011) due to the formation of more (OH^-) were in CaO NPs after pH 7.

3.8.2. Effect of adsorbent dosage

The effect of CaO NPs dosage on the adsorption of Pb (II) ion in aqueous solution was studied by varying the CaO NPs sample from 0.25 g to 1.5 g for constant initial concentration, solution pH, and contact time. It was observed that the removal efficiency increased as the adsorbent dosage of the CaO NPs increasing. The increasing of CaO NPs as an adsorbent dosage resulted in the increases in the availability of more adsorptive (binding) sites and sorptive surface area, then it leads to the increasing of Pb (II) removal efficiency at neutral pH, 105 min contact time, and 60 mg/L initial concentration of Pb (II) ion. As depicted in Fig. 7, the Pb (II) removal percentage from the aqueous solution by CaO NPs increased rapidly up to 94.33% for a dose of 0.5 g/100 mL. After that, the removal efficiency of Pb (II) increased slowly up to the value of 99.67% at a dose of 1 g/100 mL. No significant change was observed in the removal of lead (II) when the dose of an adsorbent was increased beyond the optimum dose. This is due to the saturation of the adsorption site during the adsorption process. Generally, the increase in

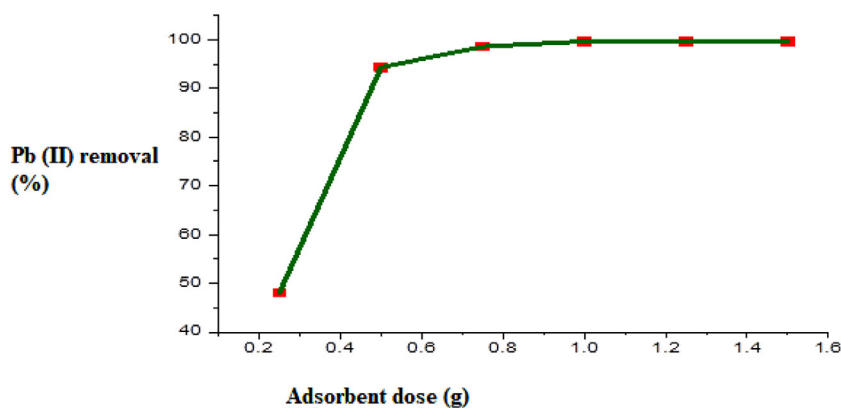


Fig. 7. Effect adsorbent dosage on Pb (II) removal.

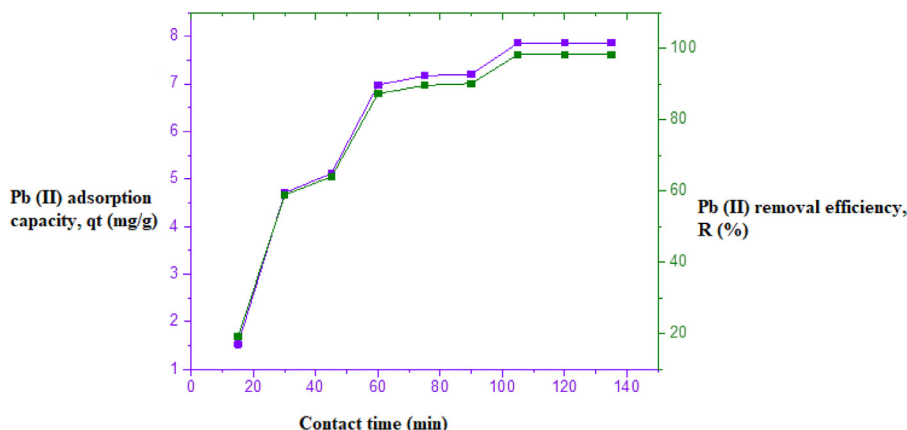


Fig. 8. Effect of contact time on Pb (II) removal.

adsorbent dosage with increase adsorption efficiency is because of the increase in adsorbent binding sites and a similar effect is investigated by (Zhang, 2012).

3.8.3. Effect of contact time

The significance of the contact time originates from the requirement for recognition of the possible rapidness of the binding and removal processes of the tested metal ions by the synthesized CaO NPs. The effect of contact times (from 15 to 135 min) of the removal of Pb (II) was shown in Fig. 8. From the obtained results, it was observed that the percentage removal of Pb (II) ion and adsorption capacity increase sharply with an increase in a contact time of the first 105 min, and a similar result was investigated in the literature (Lee Moo-Yeal, 2017). As depicted in Fig. 8, it could be concluded that as contact time increases the metal removal efficiency and metal adsorption capacity increases up to equilibrium was reached at 105 min. Further increase in contact time beyond 105 min did not enhance the Pb (II) removal efficiency and the adsorption capacity. At 105 min, 120 min, and, 135 min the %R and qt were 96.26% and 7.86 mg/g respectively.

3.8.4. Effect of initial metal concentration

The effect of initial Pb(II) concentrations ranging from 30 to 150 mg/L on adsorption was investigated and also carried out with a fixed dose of adsorbent, solution pH, and contact time of, 0.75 g, 7, and 105 min respectively. It was evident from the figure that the removal of Pb (II) percent decreased as the initial concentration of Pb (II) was increased. The Pb (II) removal efficiency was 99.66% at an initial concentration of Pb (II) of 30 mg/L and 63.8% at an initial concentration of Pb (II) of 150 mg/L. This behavior could be happened due to the limitation of active sites on the adsorbent surface. At higher concentrations, the

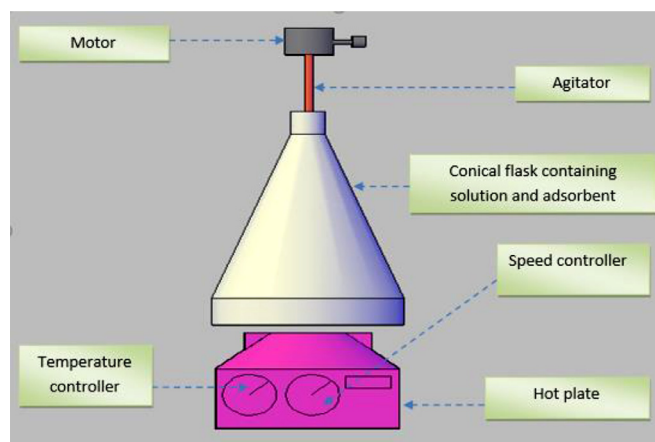


Fig. 9. Experimental Set-Up of Batch Adsorption.

metal ions are relatively higher than the available binding sites, hence, decreasing the removal percentage. This represents saturation of active sites found on CaO NPs samples for interaction with contaminants illustrating those less favorable sites were involved in the process with increasing concentration. Another cause for percentage removal decreased was in the equation $\%R = (C_0 - C_e) / C_0$, a larger increment in the denominator when compared with the numerator value. The increase in initial Pb (II) concentrations increases the interaction between Pb (II) and CaO NPs. Hence, an increase in the initial concentration of Pb (II) increases the adsorption uptake of Pb (II). This is because of the increase in the

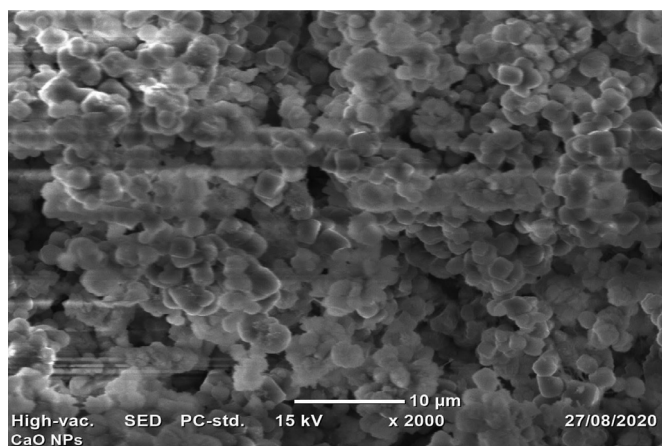


Fig. 10. SEM image of CaO NPs.

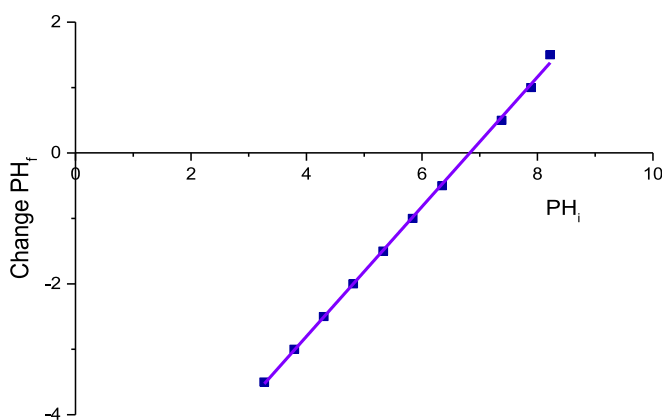


Fig. 11. Zero point charge of CaO NPs.

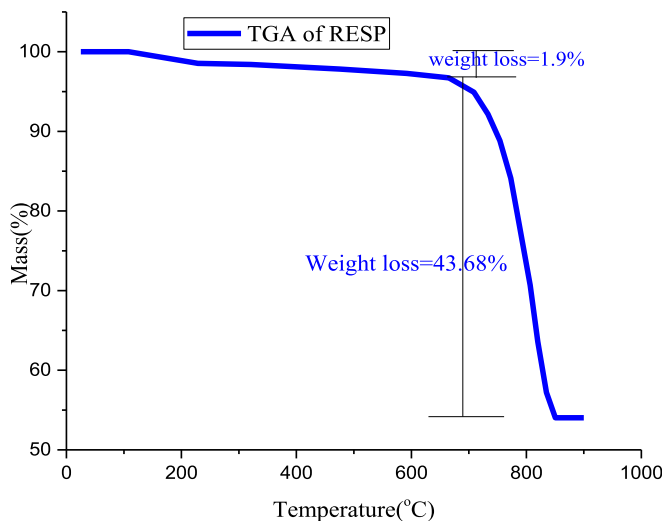


Fig. 12. TGA result of raw eggshell powder.

driving force of the concentration gradient between the increase in the Pb (II) ions concentration and adsorbent solid.

As depicted from Fig. 15 the adsorption capacity for CaO NPs was increased from 3.98 to 12.76 mg/g as the Pb (II) concentration in the test solution was increased from 30 to 150 mg/L. Therefore, the rate of adsorption and metal uptake increased with an increase in Pb (II) concentration.

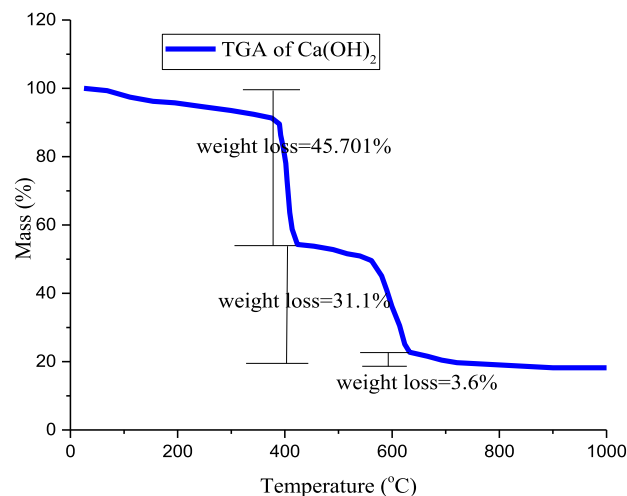


Fig. 13. TGA curve of Ca(OH)₂ gel.

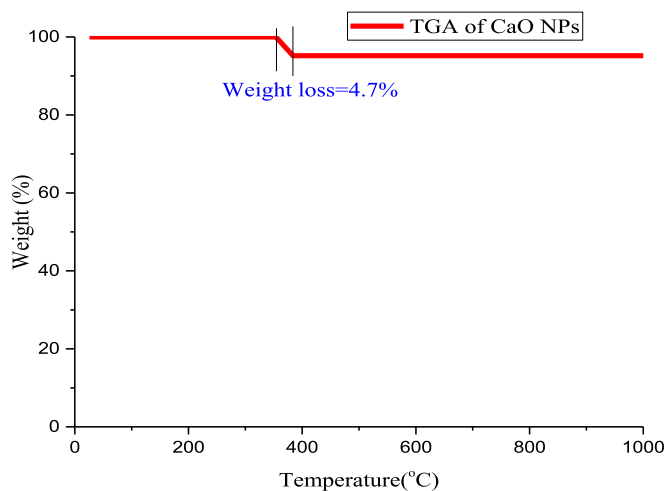


Fig. 14. TGA curve of CaO NPs.

3.8.5. Experimental results on adsorption isotherm studies

The adsorption isotherm is typically described by an isothermal equation whose parameters express the affinity and the surface property of the sorbent. The adsorption isotherm can be generated based on the theoretical models from which Langmuir, Freundlich, and Temkin models are the most used. They study the relationship between the sorbate on the surface of the sorbents that is the number of species adsorbed per unit mass of sorbent and the concentration of solute left in the solution. The possibilities of the adsorption isotherm to explain the resulted data depend on the correlation coefficients (R²).

The adsorption data can be interpreted using the relationships which describe the distribution of Pb ion between aqueous solution and solid phases. The equilibrium experiments were conducted in a 250 mL Erlenmeyer flask with 0.75 g/100 mL of CaO NPs at initial Pb (II) concentration of 30,60,90,120, and 150 mg/L under ambient temperature. The solutions were adjusted to a pH of 7.0 using 0.1 M NaOH or 0.1 M HCl. The adsorbate-adsorbent solutions were agitated at a constant speed of 250 rpm for an equilibrium time of 105 min.

Those three isothermal models can narrate metal uptake per unit mass of the adsorbent, q_e, to equilibrium sorbate concentration in the bulk fluid phases, C_e. The linear regressions of these three isotherm models were used to check the best fitting model and the suitability of the model and compared by judging the correlation coefficients. Langmuir models fitted the sorption data very well in the investigated con-

Table 5
Summary equilibrium constants and parameter values of Pb (II) with different isotherms.

Heavy metal ion	Langmuir isotherm			Freundlich Isotherm			Temkin isotherm		
	Qm (mg/g)	K _L (L/mg)	R ²	n	K _f (mg/g)	R ²	K _T (mg/L)	b _T (J/mol)	R ²
Pb (II) as total	0.877	1.48	0.9963	5.45	6.5203	0.978	176.69	1773.7	0.977

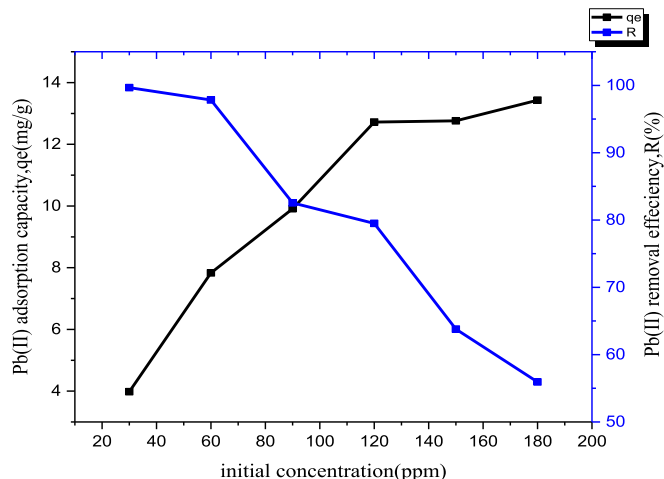


Fig. 15. Effect of initial concentration on Pb (II) adsorption.

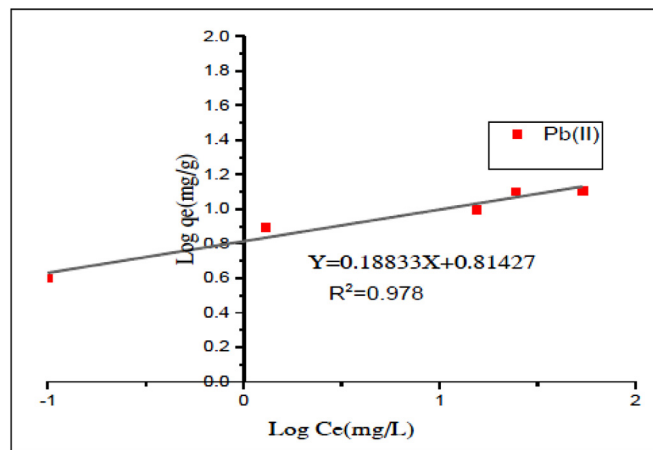


Fig. 17. Freundlich isotherm of Pb removal.

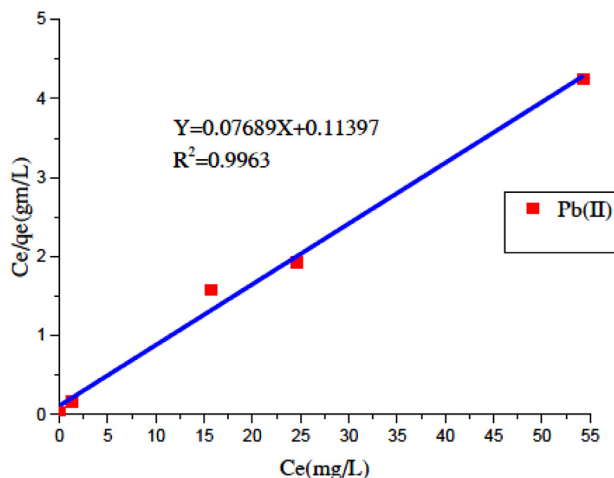


Fig. 16. Langmuir isotherm of Pb removal.

Table 6
Langmuir separation factor, R_L.

Concentration (mg/L)	Langmuir Separation factor, R _L of Pb
30	0.022
60	0.011
90	0.0074
120	0.0056
150	0.0045

centration range with a maximum correlation coefficient of R² value 0.9963 as depicted in Fig. 16. The Langmuir model assumes that the adsorptions of metallic ion (Pb) occur on a homogeneous surface by monolayer sorption with a finite number of identical sites. The Langmuir constants like K_L ($\frac{\text{intercept}}{\text{slope}}$) and qm ($\frac{1}{\text{intercept}}$) were calculated from Ce/qe versus Ce and obtained as 1.48 mg/L and 0.877 mg/g respectively. R_L = 1 / (1 + K_LC₀), since the calculated values from Table 6 was all occurred between 0 and 1.0 which clarify favorable adsorption.

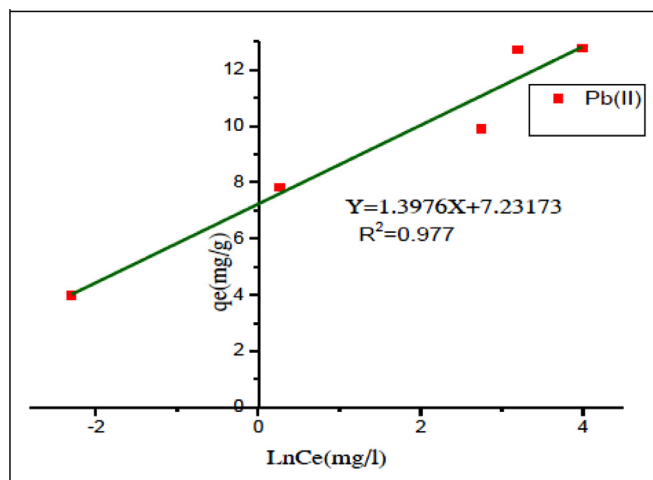


Fig. 18. Temkin Isotherm of Pb removal.

The Freundlich isotherm was an empirical interaction expressing the adsorption of solute substances from a liquid phase to a surface of the solid and assumes that different sites with several adsorption energies were involved. The model was plotted as log Ce against log qe as depicted in Fig. 17, to get the values of constants K_F and n indicating the adsorption capacity and the adsorption intensity. The Freundlich constants K_F ($10^{\text{intercept}}$) and n ($\frac{1}{\text{slope}}$) were 6.52034 mg/g and 5.455 respectively. As we observed from analysis, the Freundlich isothermal model also fitted the experimental data. But the level of its fitness was less than that of the Langmuir isotherm with a correlation coefficient, R² of 0.978. From Table 6 the value of n was found to be 5.455 showing that the CaO NPs had a heterogeneous surface since the value fulfill the heterogeneity condition of 0 < n < 10. Furthermore, the value of $\frac{1}{n}$ (0.1833) was below unity showing that a chemisorptions process.

A graph of qe against ln Ce shown in Fig. 18 was to check the validity of Temkin isotherm and to obtain the equilibrium constants K_T and b_T, where constant b_T describes the heat of adsorption (J/mol) and K_T is equilibrium binding constants (L/g) stands to the maximum binding en-

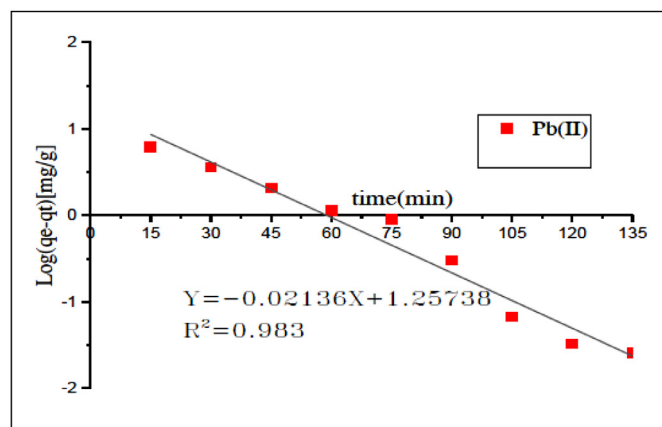


Fig. 19. Pseudo first-order kinetic model of Pb (II) adsorption.

Table 7

Kinetics Parameter's values.

Kinetics model	Parameters	Values	Correlation coefficients
Pseudo -first -order	qe(mg/g)	18.09	R ² = 0.983
	K ₁ (min ⁻¹)	0.0492	
Pseudo-second-order	qe(mg/g)	10.143	R ² =0.9982
	K ₂	0.00283	
Intra particle diffusion	Ki	0.7607	R ² =0.943
	C	- 0.0755	

ergy. The correlation coefficient obtained from the graph of Temkin was 0.977 which was smaller than the correlation coefficient obtained from Langmuir and Freundlich isotherms. And from those Langmuir isotherm scored the highest correlation coefficient (R²) and well fit the isothermal model. A similar result was investigated using copper oxide nanostructure with oval-shaped (Farghali, 2013). Therefore, it could be concluded that the Langmuir isotherm model was more suitable for the adsorption of Pb (II) ions than the Freundlich and Temkin isotherms based on the experimental study, which indicates the homogeneous distribution of active sites on CaO particle surface were shown in Table 5.

3.9. Equilibrium adsorption kinetic studies

The studies of the adsorption kinetics determine the extent of use of adsorption capacity as a function of residence time between the liquid phase and solid. Adsorption kinetics was determined by evaluating adsorption uptake of lead ions from the aqueous solutions at a various time gap of (15–135 min), remaining the other factors (parameters) constant. The solutions were adjusted to a pH of 7.0 using 0.1 M NaOH or 0.1 M HCl. The adsorbate-adsorbent solutions were agitated at a constant speed of 250 rpm with an adsorbent mass of 0.75 g/100 mL. From the laboratory, experimental work resulted from kinetics study, the pseudo-first-order, pseudo-second-order and, intra-particle diffusion were tested to determine the adsorption mechanism of Pb (II) ion onto CaO NPs. The linearized plots of their kinetic models were given in Fig. 19, 4.18 & 4.19 respectively, and calculated constants from their intercepts and slopes, and their correlations (R²) were summarized in Table 7.

The pseudo-first-order, pseudo-second-order, and intra-particle diffusion model plots revealed that the adsorption of Pb (II) onto the CaO NPs with their respective correlation coefficients. In comparison to the pseudo-first-order and intra-particle diffusion models, the pseudo-second-order model kinetic model of Pb (II) up-take showed excellent linearity with a high correlation coefficient (R²) of 0.9982. The well-fitted model of pseudo-second-order was the mechanism of Pb (II) biosorption process onto CaO NPs to be chemisorptions process, while the heavy metal ion attached to the solid(sorbent) surface by forming

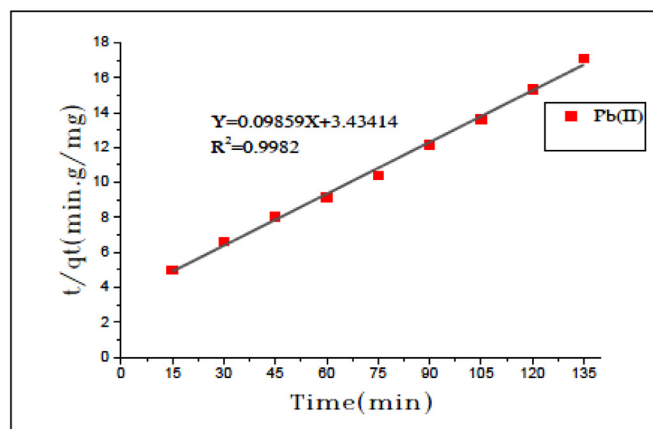


Fig. 20. Pseudo second-order kinetic model graph of Pb (II) adsorption.

covalent (chemical) bonds and have tendencies to find sites which maximize their coordination number with the surface (Wong, 2003).

The value of the correlated coefficient of the pseudo-first-order model was lower than that of the pseudo-second-order model and also a large difference in equilibrium adsorption capability (qe) between the calculated and experimental data was resulted, telling a poor pseudo-first-order fit to the experimental data as shown in Fig. 20.

In general, the kinetics of Pb (II) ions adsorption onto CaO NPs obeyed the pseudo-second-order model, which recommends chemisorptions as the rate-limiting step in the adsorption process involving valence forces through exchange or sharing of electrons between sorbent and sorbate.

The fitness of the pseudo-second-order model for Pb (II) adsorption experimentally was matched with other different scholars' studies. (Senthil Kumar, 2010) studied the adsorption of lead (II) from aqueous solutions using nano-solvent coated activated carbon. (Wong, 2003) analyzed the removal of Pb (II) by batch experiment using rice husk. (Farghali, 2013) studied the adsorption of Pb (II) ions from aqueous solutions using copper oxide nanostructure. And (Yahaya, 2016) examined the removal of Pb (II) from the wastewater using cocoa pod husk. Through these all researchers' investigations, the pseudo-second-order model explained kinetics of reaction better than the pseudo-first-order model with evidence of higher correlation coefficients.

It is essential to study the desorption of Pb (II) ions from the material because of the adsorbed Pb (II) ions may not only be separated from the Pb (II)-CaO NPs, but the material may also be regenerated to continue adsorbing Pb (II) ions. The results indicated that the Pb(II)-CaO NPs were re-usable and stable for Pb(II) adsorption. To treat waste water, regeneration of the adsorbent material plays an important role in economic development as it helps to protect the environment and recycle the adsorbent (Pb(II) and adsorbent (activated carbon) ions. Successful application of the technique also reduces dependence on thermal activation, incineration and landfill, directly or indirectly increasing environmental pollution. Desorption studies help in process design systems by providing information on the mechanism and recovery of adsorbents from industrial wastewater and adsorbent Fig. 21.

3.10. Statistical and graphical analysis of experimental results

3.10.1. Analysis of variance (ANOVA)

Analysis of variance (ANOVA) was used to evaluate the statistical significance of the quadratic model. The significance of the model and the model terms are decided by using the F-test and p-test. The higher the magnitude of F and the smaller pvalue, the more significance is the conforming model and model terms. The application of design expert software was to design the experiments and randomize the runs. Randomization makes the process parameters (factors) in one run neither

Table 8
Analysis of variance (ANOVA) for response surface quadratic model of Pb (II) ions up-take.

Source	Sum of Squares	Df	Mean Square	F-value	p-value	Comment
Model	14,535.21	14	1038.23	246.08	< 0.0001	Significant
A-concentration	2488.81	1	2488.81	589.90	< 0.0001	Significant
B-pH	7200.96	1	7200.96	1706.78	< 0.0001	Significant
C- dosage	983.81	1	983.81	233.18	< 0.0001	Significant
D-Contact time	1180.20	1	1180.20	279.73	< 0.0001	Significant
AB	0.0400	1	0.0400	0.0095	0.9237	Not significant
AC	0.1980	1	0.1980	0.0469	0.8314	Not significant
AD	4.93	1	4.93	1.17	0.2969	Not significant
BC	286.12	1	286.12	67.82	< 0.0001	Significant
BD	53.73	1	53.73	12.73	0.0028	Significant
CD	0.2756	1	0.2756	0.0653	0.8017	Not significant
A ²	64.33	1	64.33	15.25	0.0014	Significant
B ²	1831.48	1	1831.48	434.10	< 0.0001	Significant
C ²	689.55	1	689.55	163.44	< 0.0001	Significant
D ²	317.58	1	317.58	75.27	< 0.0001	Significant
Residual	63.29	15	4.22			
Lack of Fit	50.70	10	5.07	2.01	0.2275	Not significant
Pure Error	12.59	5	2.52			
CORE TOTAL	14,598.50	29				

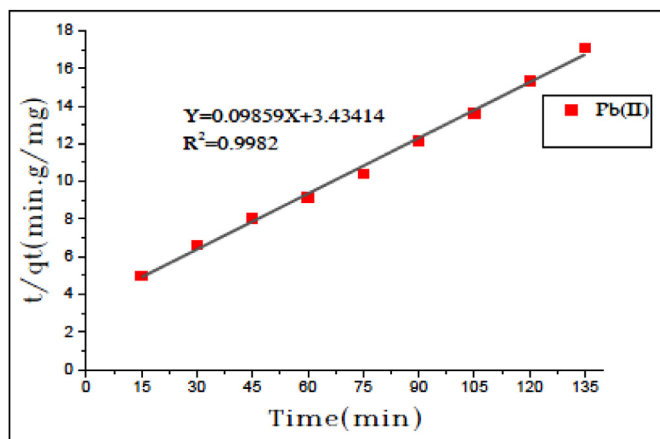


Fig. 21. Intra particle diffusion kinetic model for Pb (II) adsorption.

depend on the process variables of the former runs nor predict the conditions in the successive run. The different process parameters such as initial metal concentrations, solution pH, adsorbent dosage, and contact time in the adsorption percentage of Pb (II) were generated in the model and optimized by response surface methodology.

Adequacy and significance of the quadratic model were determined by analysis of variance (ANOVA). It was found that the model was statistically significant at the F-value of 246.08 and the value of $P < 0.05$. The parameters which have p-probability of statistics value less than 0.05 were always significant. From this current study, the probability of model p statistics was < 0.0001 illustrating that the model suggested by the software was highly significant. In this case, all four linear terms, the interaction of solution pH and adsorbent dosage, the interaction of pH and contact time, and second-order terms of all individual effects (A, B, C, D, BC, BD, A², B², C², D²) were statistically significant ($P < 0.05$). The p values greater than 0.10 indicate the model terms are not significant. The lack of Fit F-value of 2.01 implies it is not significant relative to the pure error. The non-significant value of lack of fit for the model implies that the developed model is valid. It is concluded that, the smaller the P-values and the larger the F-value the more significant is the corresponding models and regression coefficients. The values of Prob $> F < 0.05$ indicate a significant regression at a 95% confidence interval as shown in Table 8.

The regression coefficient and the corresponding confidence interval of 95% (CI) interval low and high were depicted in Table 9. If zero (0) was in the list of low and high 95% CI, the factors have no effects. Therefore, from the below table it could be judged that the regression coefficients of initial concentration, pH, dosage, contact time, and the combined effects of all have a highly significant effect on Pb(II) adsorption process.

The determination coefficient of (R^2) was used to ensure the accurateness of the model. The determination coefficient ($R^2 = 0.9957$) revealed that the model cannot explain only 0.43% of the total variable. From Table 10 above, the R^2 of 0.9957 was in reasonable agreement with the Adjusted $R^2 = 0.9916$, their difference was less than 0.2. The regression coefficient (R^2) quantitatively examines the relatedness between experimental and predicted responses. Results of $R^2 = 0.9957$ and $Adj-R^2 = 0.9916$ resulted explain that the predicted values were found to be in good agreement with the experimental values. Seeing that the R^2 value is nearer to one, it shows that the regression line exactly fits the data. Generally, the model best of fit was checked by regression coefficient (R^2) and it also suggests good adjustment to the experimental results. The adjusted determination coefficient, $Adj-R^2 = 0.9916$ was adequate for proving the significance of the model. Predicted- R^2 indicating that the model explains a high percentage of 0.9788 of variability. Adequacy model precision gives the ratio of the signal to the noise. The ratio determined was greater than 4 is desirable and the Adequacy precision of 59.2981 indicates an adequate signal as shown in Table 11. This model can be used to navigate the design space. A low value of the variation coefficient ($CV = 2.97$) shows the reliability of the experiments.

The final equation in terms of coded factors:-

$$\begin{aligned} \text{Pb(II)\%Removal} = & 83.57 - 10.18 * A + 17.32 * B + 6.40 * C \\ & + 7.01 * D + 0.050 * A * B \\ & + 0.1113 * A * C + 0.5550 * A * D - 4.23 * B * C \quad (24) \\ & - 1.83 * B * D - 0.1312 * C * D - 1.53A^2 \\ & - 8.17 * B^2 - 5.01 * C^2 - 3.40 * D^2 \end{aligned}$$

The Eq. (24) illuminates how the lead metal adsorption onto sol-gel-based synthesized CaO NPs was affected by individual factors (linear and quadratic) or double interactions. Those negative coefficient values showed that individual or double interaction factors negatively affect Pb (II) adsorption while positive coefficient values represent the factors that increase Pb (II) removal efficiencies. From the equation above, among all linear factors, initial metal concentrations had a negative effect, but pH, adsorbent dosage, and contact time had a positive effect

Table 9
Regression coefficients and the corresponding 95% CI (Low and High).

Terms	Coefficient estimate	Standard error	F-value	P-value	95% CI Low	95% CI High
Intercept	83.57	0.8386			81.78	85.36
A-concentration	-10.18	0.4193	246.08	< 0.0001	-11.08	-9.29
B- pH	17.32	0.4193	589.90	< 0.0001	16.43	18.22
C-Dosage	6.40	0.4193	1706.78	< 0.0001	5.51	7.30
D-contact time	7.01	0.4193	233.18	< 0.0001	6.12	7.91
AB	0.0500	0.5135	279.73	< 0.0001	-1.04	1.14
AC	0.1113	0.5135	0.0095	0.9237	-0.9833	1.21
AD	0.5550	0.5135	0.0469	0.8314	-0.5395	1.65
BC	-4.23	0.5135	1.17	0.2969	-5.32	-3.13
BD	-1.83	0.5135	67.82	< 0.0001	-2.93	-0.7380
CD	-0.1312	0.5135	12.73	0.0028	-1.23	0.9633
A ²	-1.53	0.3922	434.10	< 0.0001	-2.37	-0.6955
B ²	-8.17	0.3922	163.44	< 0.0001	-9.01	-7.34
C ²	-5.01	0.3922	75.27	< 0.0001	-5.85	-4.18
D ²	-3.40	0.3922	434.10	< 0.0001	-4.24	-2.57

Table 10
Model adequacy measures.

STD. Dev.	2.05	R-Squared	0.9957
MEAN	69.07	ADJ R-Squared	0.9916
C.V. %	2.97	PRED R-Squared	0.9788
PRESS	310.16	ADEQ Precision	59.2981

on lead removal. Therefore positive values favored the optimization of the process conditions.

3.10.2. Graphical analysis of one factor and interaction effects on ANOVA

Usually, it is significant to check the fitted model to ensure an adequate approximation to the real system. Different diagnostic model plotted were normal probability plot which compares the distribution of residuals along the straight line (the normal distribution). Tolerate some scatter even with normal data. Our center of attention only on definite patterns like an S-shape curve, which points out the transformation of responses, may afford a better analysis. The residuals versus predicted plots checks for continuous (constant) variance across the ranges of prediction. Variances that are not constant are illustrated as upward or downward patterns. If the plot has arbitrarily scattered between red lines and then the assumption of constant variance is established.

The predicted versus actual indicating that all the data points were distributed along the 45° line, indicating that the model can provide an acceptable fit for experimental data. Similar results are obtained by (Okolo, 2020). This shows both the actual experiment and the predicted values were approximate and the model satisfies the assumption of analysis of variance (ANOVA), i.e. the error distribution was approximately normal.

The normal plots versus residuals used in judging whether the models are satisfactory. The figure indicated that the data were plotted against a theoretical normal distribution, and the points should form an approximately straight line and a departure from this line would point out the departure from a normal distribution. From this graphical result, the data points were very small deviating from the normal distribution given, but not very critical Fig. 22.

If the model is correct and the assumptions are met, the residue is not expected to be structured. It is also unrelated to any other variables including the predicted response. A simple check is to plot residual versus predicted (fitted) values. A plot of residuals versus the rising predicted response value tests the assumption of constant variances. The plot shows random scatter which indicating no need for an alteration to minimize personal error as shown in Fig. 23.

3.10.3. Estimation of the quantitative effects of the factors

The objectives of the CCD method applied in this study was to find out the significant effect of the process variables on the percentage removal of Pb (II) on 3D response surface and contour plots and were used to study the effect of all factors on the response. Model analysis of response surface plots and contour plots were the graphical representations of the regression equations used to study the relationship between the response and experimental levels of each factor. The 3-D response surface and contour plot for Pb (II) removal percentage versus any two independent factors by putting the other independent factors at medium level. The 2-D contour plot is a graphical representation of the response across the factors displayed on an axis. The 3-D surface plot is a projection of the contour plot providing shape as well as the color and contour.

There were two effects, single (main) and interaction effects which were studied by using a design expert graph. The single effects in the linear model further studied by considering one-factor change within a range beginning from lower level to higher level, making the other factors at a medium level (center point). As it was illustrated, the removal percentage of Pb (II) ions decreased with increasing initial concentrations. The maximum percentage removal, 79.558% was obtained at 60 mg/L and the minimum percentage removal, 58.78% was obtained at 120 mg/L. For pH, minimum reduction percentage, 51.81% resulted at pH=3, and maximum removal percentage, 86.5% resulted at neutral pH. This is because as pH increases, the adsorbent surfaces become less protonated and stronger attraction of cationic species of Pb (II). In the acidic pH, the most common species of Pb (II) cations were: Pb²⁺, Pb(OH)⁺, and Pb(OH)²⁺, hence under acidic conditions the adsorbent's surface becomes protonated, consequently, there is a decrease in the

Table 11
Model summary statistics.

Source	Sequential p- value	Lack of Fit p-value	Adjusted R ²	Predicted R ²	Comment
Linear	< 0.0001	0.0002	0.7819	0.7492	
2FI	0.8321	< 0.0001	0.7491	0.7151	
Quadratic	< 0.0001	0.2275	0.9916	0.9788	Suggested
Cubic	0.0868	0.6982	0.9959	0.9796	Aliased

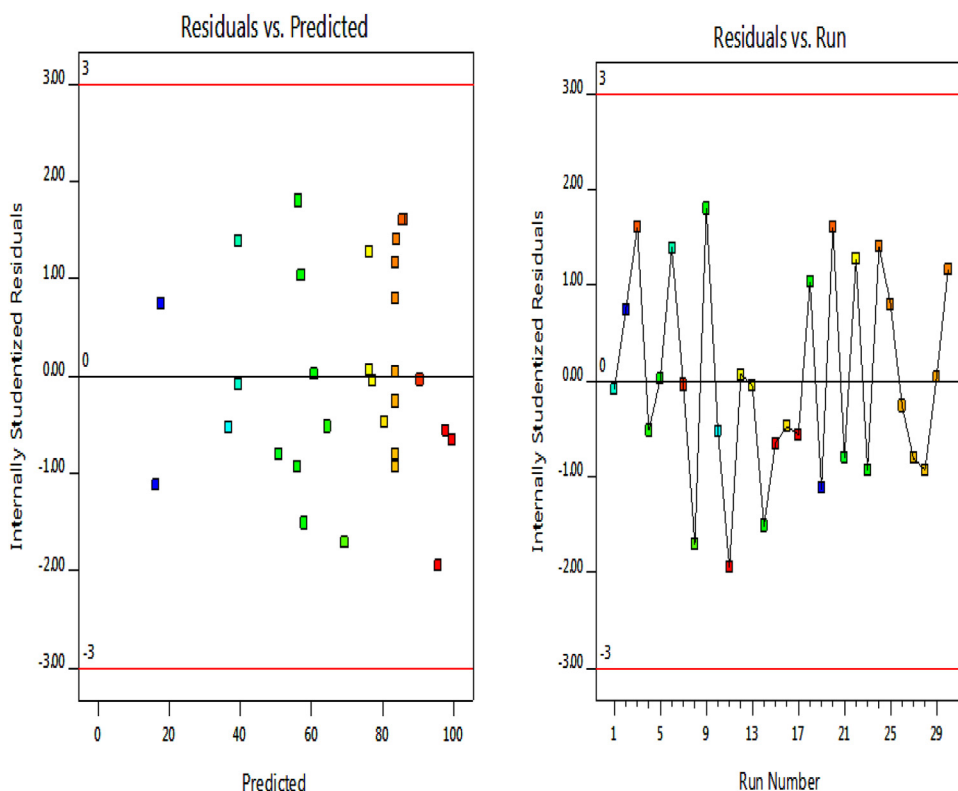


Fig. 22. Diagnostic plot model for Pb (II) adsorption on CaO NPs .

electrostatic attraction between Pb (II) and the surface of the adsorbent, with a decrease in adsorption percentages (Okolo, 2020).

For adsorbent dosage minimum removal percent, 62.7% was obtained at a minimum dosage (0.5 g), and maximum removal percentage, 75.59% was obtained at higher adsorbent dosage (1 g). This is because of the larger accessibility of active sites. In the case of contact time against removal, percentage reveals a direct relationship until the equilibrium of removal percentage attains. From the one factor revealed below, the minimum removal percentage, 62.11% was obtained at a contact time of 45 min, and the maximum removal percentage, 76.21% was obtained at the contact time, 105 min.

3.11. Interaction effects of initial Pb (II) concentrations and solution pH (AB)

Interaction effect of initial concentration and pH on removal efficiency of Pb (II) at a medium level (center point) of the contact time (75 min) and adsorbent dosage (0.75 g/100 mL) was examined. The percentage removal of Pb (II) ion increased with decreasing initial concentrations of Pb (II) and increased pH of the solution. As shown from the from Fig. 24, the removal efficiency increases with increasing from pH, 3 to 6.856. At pH 6.856 and an initial concentration of Pb (II), of 104.35 mg/L, the adsorption efficiency obtained was 87.1%. But in the same pH, and 66.8 mg/L initial concentration of Pb (II) the adsorption % obtained was 99.55%. The maximum removal efficiency of very high was observed at constant adsorbent dosage (0.75 g/100 mL) and contact time (75 min).

3.12. Interaction effects of initial lead (II) concentration and adsorbent dosage (AC)

interaction effects of initial Pb (II) concentration and adsorbent dosage on the removal percentage was illustrated. It can be observed that the decrease in initial Pb (II) ions concentration and the increase in adsorbent dosage resulted in an increase in removal percent of Pb (II).

The plot also showed that a higher pH value and the variation contact time have more effect on the percent removal of Pb (II) than the initial metal concentrations were shown in Fig. 25. This was why, at the beginning phase where the surface adsorbent vacant site was empty, the adhering probability is very high and adsorption takes place at a higher rate. And then after the adsorption rate was becoming slow due to the saturation of binding sites. 93.8% of removal of the Pb(II) was obtained at an initial concentration of Pb(II) of 63.02 mg/L and adsorbent dosage of 0.96 g, and the rest two variables at their medium level.

3.13. Interaction effects of initial lead (II) concentration and adsorbent dosage (AC)

The interaction effects of initial Pb (II) concentration and adsorbent dosage on the removal percentage was illustrated. It can be observed that the decrease in initial Pb (II) ions concentration and the increase in adsorbent dosage resulted in an increase in removal percent of Pb (II). The plot also showed that a higher pH value and the variation contact time have more effect on the percent removal of Pb (II) than the initial metal concentrations were shown in Fig. 26. This was why, at the beginning phase where the surface adsorbent vacant site was empty, the adhering probability is very high and adsorption takes place at a higher rate. And then after the adsorption rate was becoming slow due to the saturation of binding sites. 93.8% of removal of the Pb(II) was obtained at an initial concentration of Pb (II) of 63.02 mg/L and adsorbent dosage of 0.96 g, and the rest two variables at their medium level.

3.14. Interaction effects of initial metal ion concentrations and contact time (AD)

combined effects of initial Pb (II) concentration and contact time on the percent removal of Pb (II) were evaluated. From the analysis, the percent removal of Pb (II) increases as initial Pb (II) concentration decreases, and contact time increases as depicted in Fig. 27. A maximum removal percentage of Pb (II), 95.04% occurred at a contact time of

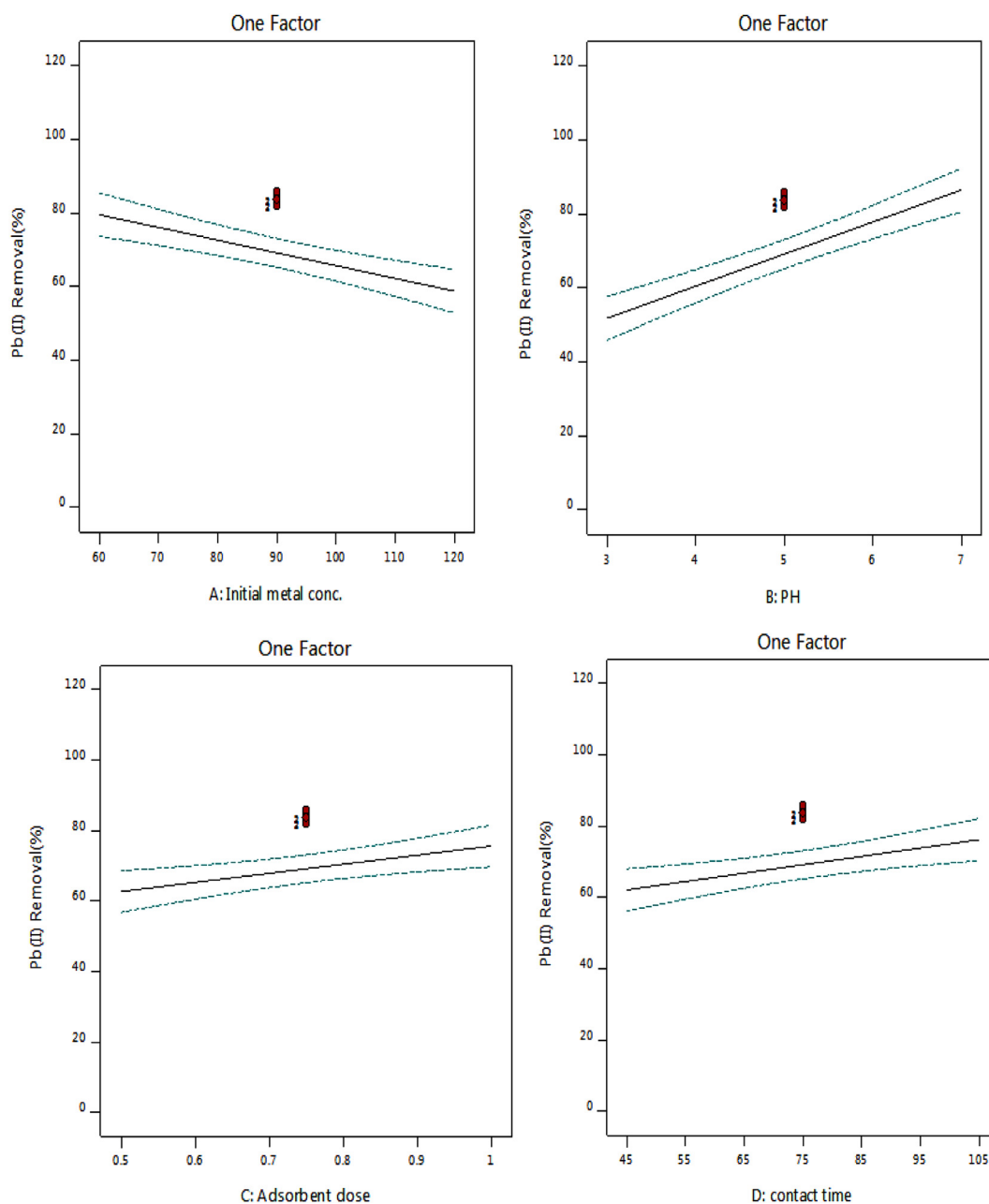


Fig. 23. Single effect of individual factors of Pb (II) removal.

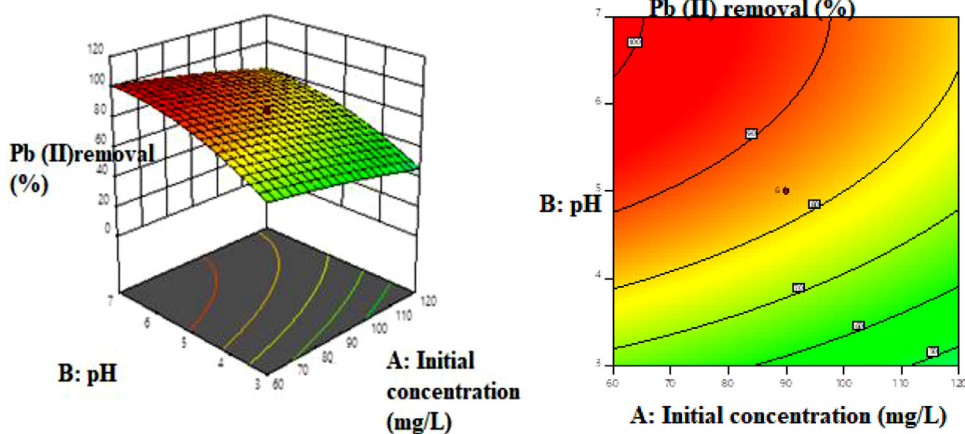


Fig. 24. Combined effect of pH and initial concentration of Pb (II) removal A) 3D Response surface plot B) contour plot.

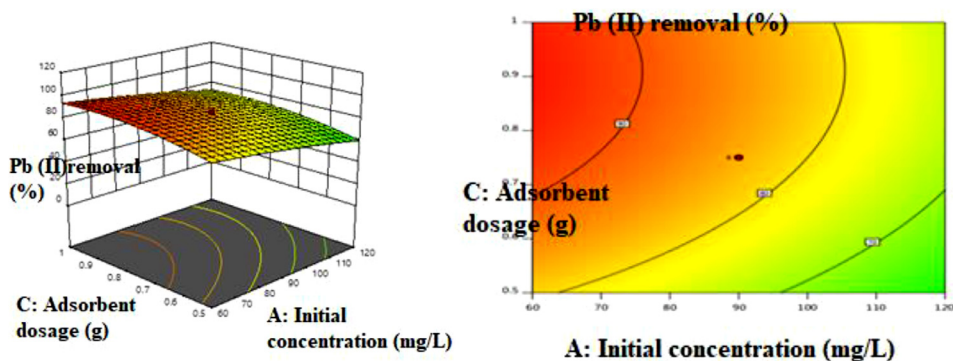


Fig. 25. combined effect of initial concentration and adsorbent dosage on Pb (II) removal A) 3D response surface plot B) Contour plot.

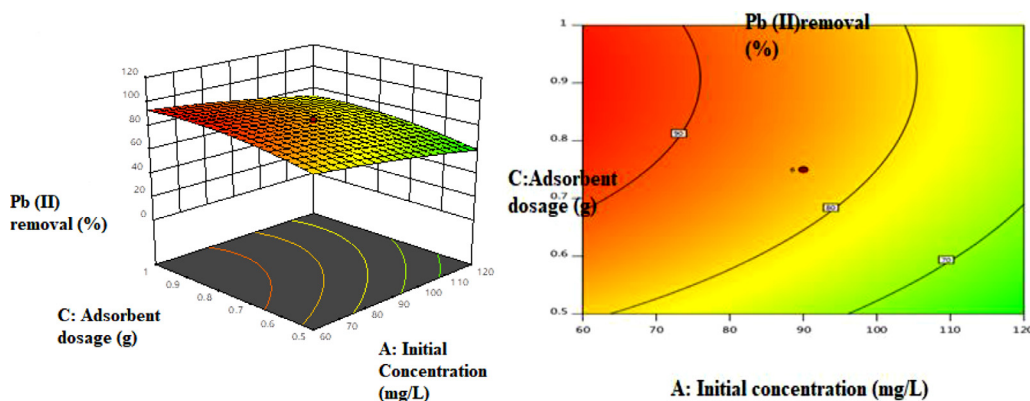


Fig. 26. Combined effect of initial concentration and adsorbent dosage on Pb (II) removal A) 3D response surface plot B) Contour plot.

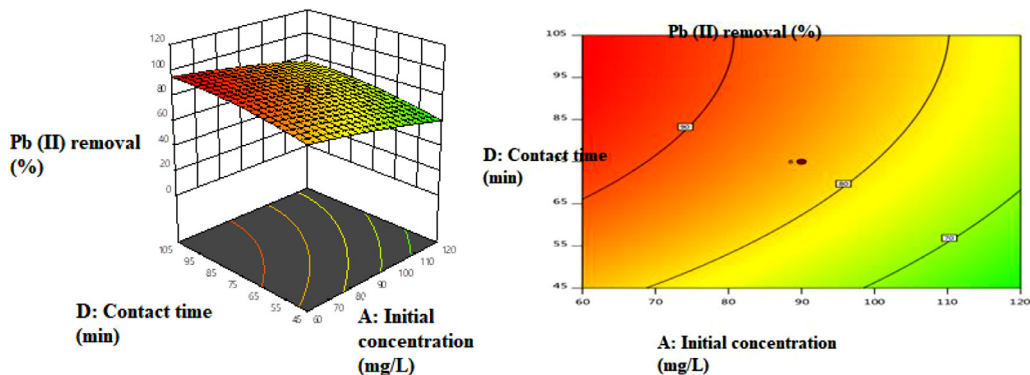


Fig. 27. Combined effect of initial concentration and contact time on Pb (II) removal A) 3D Response surface plot B) Contour plot.

104 min and an initial Pb (II) concentration of 61.5 ppm. In general, the adsorption rate was higher at initial contact time as enough number of active sites was available for adsorption. But through time, a higher amount of Pb (II) ion got adsorbed on the CaO NPs surface and therefore, the surface area decreased.

3.15. Optimization parameters of lead (Pb (II)) removal by CaO NPs

The optimization was conducted after interaction effects between adsorption parameters. Those optimum working conditions of the possible goals of numerical optimizations were maximized, minimize, target, in range of the response (percentage removal of Pb (II)) and factors only (initial metals concentration, pH, adsorbent dosage, and contact time) which applied for the analysis of optimization. The targeted criterion was maximizing percentage removal of Pb (II) and while the other factors remaining in range. Design-Expert software version 11.1.0.1 was generated a set of solution to determine the optimum conditions which

had high composite desirability and removal efficiency. Desirability is the objective function. For any given response it ranges from zero to one. The value of one in desirability indicates the ideal case while zero represents one or more responses fall outside the desirable limit.

The need for numerical optimization is to bring into being a maximum response for all of the runs analyzed under these conditions. The experimental percentage and predicted percentage values with percent removal of Pb (II) were explained below under validation experiments. A very small difference in percent between the experimental and predicted removal percentages of Pb (II) shows sufficient to predict the Pb (II) removal process using the adsorbent CaO NPs in the ranges of factors studied as depicted in Table 12.

3.16. Validation experiments

The target of numerical optimization is to generate the maximum response for all of the runs analyzed. To confirm the optimization results,

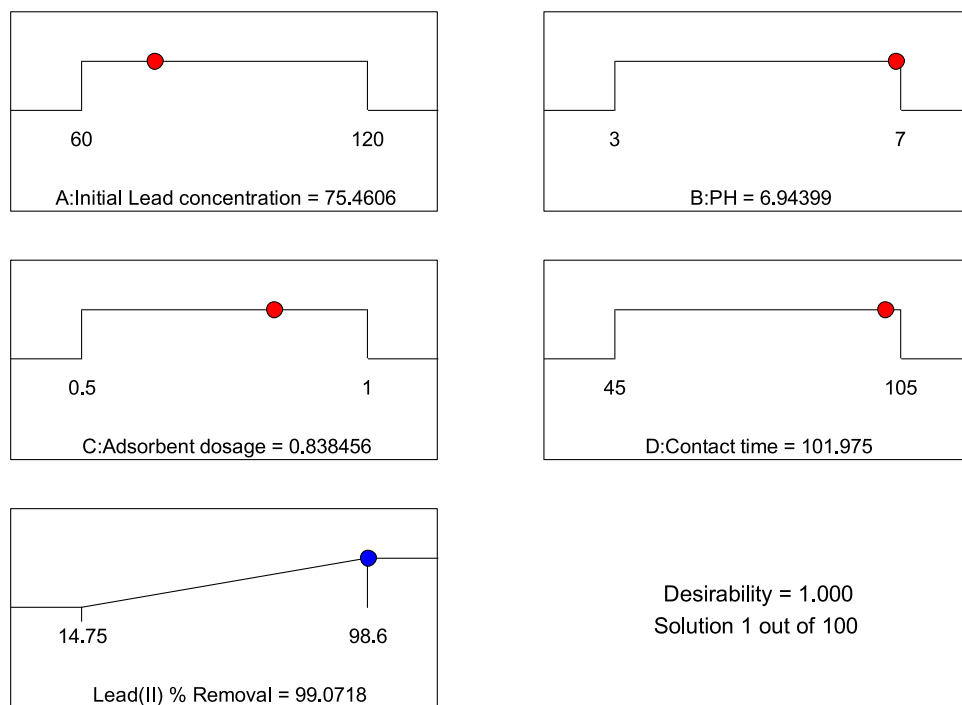


Fig. 28. Desirability ramp for numerical optimization for the selected variables using CaO NPs.

Table 12
Goals of the optimization and its ranges.

Variables	Ultimate goal	Experimental range	
		Lower limit	Upper limit
Initial Pb (II) concentration (mg/L)	In range	60	120
pH	In range	3	7
Adsorbent dosage (g/100 ml)	In range	0.5	1
Contact time (min)	In range	45	105
% removal of Pb (II)	maximize	14.75	98.6

Table 13
Optimum conditions and model validation.

Variables	Optimum results
Initial Pb(II) concentrations (mg/L)	75.46
pH	6.94
Adsorbent dosage(g/100 ml)	0.838
Contact time (min)	101.97
% removal of Pb(II)	99.07
Experimental % removal of Pb(II)	98.86
Desirability	1

the experiment was conducted under predicted conditions through the developed model. The model predicted 99.07% removal of Pb (II) at concentration 75.46 mg/L, pH 6.94, adsorbent dosage 83.8 g/L, and contact time 101.97 min. Also, the experimental value obtained at these conditions of Pb (II) removal was 98.86% and was in close agreement with the result obtained from the model and hence validated the findings of the optimization. This experimental validation was the final step in the modeling process to investigate the accuracy of the established models. The results of predicted and experimental values of the output variables were evaluated in Fig. 28 and concluded in Table 13. The maximum error (%) between the predicted and the experimental values was 0.21%, which is less than 3%, indicating that the quadratic models adopted could predict the experimental result well (Okolo, 2020). Hence, it was concluded that the models accurately represent lead (II) ion removal over the experimental range studied.

Figure 1, 4, 9, 10, 11, 12, 13, 14, 15, 16, 18, 19, 20, 21, 22, 23, 24, 25, 26, 27 and 28, 4, 9–28; Table 1, 2, 3, 5, 6, 7, 8, 9, 10, 11, 12 and 13, 5–13

4. Conclusions

In this study, lead ion removal from aqueous solution using sol-gel derived calcium oxide nanoparticles, which were utilized as an effective and inexpensive sorbent for heavy metal removal particularly lead ions was investigated. The CaO NPs derived from low-cost waste hen eggshells become a better adsorbent because it has low moisture contents (0.135%), therefore the adsorbent could be stored for a long time devoid of any preservations. The synthesized CaO particles from waste hen eggshell ensured an important increase in the specific surface area of (77.4m²/g).

Batch mode experiments were applied to study the effect of initial metal concentrations, pH, adsorbent dosage, and contact time using central composite design expert 11.1.0.1. It was found that the percent adsorption of Pb (II) decreased with an increase in initial Pb (II) concentration. This case was since for a fixed adsorbent dosage, the overall available active sites were limited as a consequence leading to a decrease in removal percentage of the adsorbate, equivalently to an increase in initial adsorbate concentration. Using the central composite design, the optimum parameter conditions of 75.46 mg/L initial Pb (II) concentration, 0.838 g adsorbent dosage, pH 6.94, and contact time 101.07 min were determined to yield a maximum Pb (II) removal of 99.07%.

The adsorption data were also used to investigate the adsorption isotherm models and kinetics models. The removal process was analyzed by Langmuir, Freundlich, and Temkin isotherm models. Langmuir’s model fitted very well to the data with correlation coefficients (R²) of 0.9963.

Kinetic models analysis for the Pb (II) removal process was conducted through pseudo-first-order, pseudo-second-order, and intra-particle diffusion models. The pseudo-second-order model was fitted very well with the highest correlation coefficient (R²) of 0.9982. ANOVA results imply that the models developed for adsorption of Pb (II) ions onto CaO NPs were highly significant based on low P values.

Declaration of statement

Jimma University in collaboration with Adama University were the sponsor of the work.

Mr. Reta Garoma was the recipient of 60,000 ETB.

Supplementary materials

Supplementary material associated with this article can be found, in the online version, at doi:10.1016/j.envc.2021.100193.

Reference

- Adeyeye, I.E., 2009. Comparative study on the characteristics of eggshells of some bird species. *Bul. Chem. Soci. Ethiopia*. 23, 159–166.
- Afroze, S., Sen, T., 2018. A review on heavy metal ions and dye adsorption from water by agricultural solid waste adsorbents. *Wat. Air Soil Pollut.* 225–229.
- Ajala, O.E., Eletta, A.A.O., Ajala, A.M., Oyeniya, K.S., 2018. Characterization and evaluation of chicken eggshell for use as a bio-resource. *J. Eng. Technol. Environ.* 26–40.
- Amare, A., 2019. Corporate environmental responsibility in Ethiopia: a case study of the Akaki River Basin. *Ecosyst. Health Sustain.* 57–66.
- Ashok, K., Jadhav, J., Panickal, S., Marathe, S., 2015. On the possible cause of distinct El Niño types in the recent decades. *Sci. Rep.* 5, 17009. doi:10.1038/srep17009, (2015)https://doi.org/.
- Beksissa, R., Tekola, B., Ayala, T., Dame, B., 2021. Investigation of the adsorption performance of acid treated lignite coal for Cr (II) removal from aqueous solution. https://doi.org/10.1016/j.envc.2021.100091 *Elsevier*.
- Bhaumik, N.K.M.R., B.Das, P.Roy., K.C.Pal., C.Das., Banrjee, A., Datta., J.K., 2012. Eggshell powder as an adsorbent for removal flouride from an aqueous solution. Equilibrium, kinetics and thermodynamic studies. *E- J. Chem.* 1457–1480.
- Blázquez, G., M., A.M.L., Tenorio, G., Calero, M., 2010. Batch biosorption of lead (II) from aqueous solutions by olive tree pruning waste: equilibrium, kinetics and thermodynamic study. *Chem. Eng. J.* 170–177.
- Boyaci, I.H., 2005. A new approach for determination of enzyme kinetic constants using response surface methodology. *Biochem. Eng. J.* (25) 55–62.
- Castro, J.C., 2011. Alternative low-cost adsorbent for water and wastewater decontamination derived from eggshell waste: an overview. *Waste Biomass Valor* 2, 157–167.
- Dagmawi, M., Mekibib, D., 2013. Chromium removal from modjo tannery wastewater using moringa stenopetala seed powder as an adsorbent. *Water Air Soil Pollut.* 221–210.
- Farghali, M.B., Enaiet Allah, A., Khedr., M.H., 2013. Adsorption of Pb(II) ions from aqueous solutions using copper oxide nanostructures. *J. Bas. Appl. Sci.* 61–71.
- Getasew Ketsela, Z.A., Alemu, T., 2020. Adsorption of lead (II), Cobalt (II) and Iron (II) from aqueous solution by activated carbon prepared from white lupine (GIBITO) HSUK. *J. Therm. Cat.* 2157–7544.
- Ghaneian, M.T., Bhatnagar, A., Ehrampoush, M.H., 2017. Biosorption of hexavalent chromium from aqueous solution onto pomegranate seeds: kinetic modeling studies. *Int. J. Environ. Sci. Technol.* 331–340.
- Gregorio Crini, E.L., D.Wilson., Lee, Morin-Crini., Nadia, 2019. Conventional and non-conventional adsorbents for wastewater treatment. *Environ. Chem. Lett.* 17, 195–213.
- Gupta, V.K., 2011. Removal of Pb(II) and Chromium from waste water using bagasse fly ash-a sugar industry waste. *J. Colloid Interface Sci.* 321–328.
- Ho, Y.S., McKay, G., 1999. The sorption of lead(II) ions on peat. *J. Wat. Resour.* 33 (32), 578.
- Igwe, Isaac O., 2007. Uptake of aromatic solvents by polyethylene films. *J. Appl. Poly. Sci.*
- Jonas, Bayuo., K., B.P.B., Abukari., Moses Abdullai, 2019. Optimization of adsorption parameters for effective removal of Lead (II) from aqueous solution. *Phys. Chem. Indian J.*
- Kaushal, A., Singh., SK., 2017. Adsorption phenomenon and its application in removal of lead from waste water: a review. *Int. J. Hydrol.* 2 issue.
- Kumaraswamy, K., Dhananjayulu, B.V., Vijetha, P., Kumar, Y., 2015. Kinetic and equilibrium studies for the removal of chromium using eggshell powder. *Res. J. Pharmac. Biol. Chem. Sci.* 529–532.
- Lalit, H., N., S., Mulatu, Dure, Thenepalli, Thriveni, Chilakala, Ramakrishna, Ahn., Ji Whan, 2019. Synthesis of nano-calcium oxide from waste eggshell by sol-gel method. *Sustainability*.
- Latif., EL., M., M., Ibrahim, A.A., El-Kady, M.M.F. 2010. Adsorption equilibrium, Kinetics and Thermodynamics of methylene blue from aqueous solutions using biopolymer oak sawdust composite. *J. Env. Sci.* 6 (6), 267.
- Lee Moo-Yeal, L.S.H., Hyun-Jae., Shin, Toshio, Kajuchi, Ji-Won., Yang, 2017. Characteristics of lead removal by crab shell particles. *Process Biochem.* 33, 749–753.
- Malik, M., Nitiss, K.C., Enriquez-Rios, V., Nitiss, J.L., 2006. Roles of nonhomologous end-joining pathways in surviving topoisomerase II-mediated DNA damage. *Mol. Cancer Ther.* 5 (6), 1405–1414.
- Ohmi, Kazuo., Sanjeeb Prasad Panday., 2009. Particle tracking velocimetry using the genetic algorithm. *J. Vis. (Springer)*.
- Okolo, B.I., E., O.O., Chinedu, M., Agu, O., Adeyi, K., Nwoso-Obieogu, K., Akatobi, N., 2020. Adsorption of lead(II) from aqueous solution using Africa elemi seed, mucuna shell and oyster shell as adsorbents and optimization using Box–Behnken design. *J. Appl. Wat. Sci* 10, 201.
- Ringot, D., Lerzy, B., Chaplain, K., Bonhoure, J.P., Auclair, E., 2007. In vitro biosorption of ochratoxin A on the yeast industry by-products: comparison of isotherm models. *Bio. Res. Technol.* 1812–1821.
- Safatian, F., 2019. Lead ion removal from water by hydroxyapatite nanostructures synthesized from egg shells with microwave irradiation. *Appl. Wat. Sci.* 9–108.
- Sanjay, S., Kolekar, M.A., 2014. Removal of malachite green dye from aqueous solution with adsorption technique using Limonia acidissima (wood apple) shell as low-cost adsorbent. *Arab. J. Chem.*
- Senthil Kumar, P., C., V., Kirthika, K., Sathish Kumar., K., 2010. Kinetics And equilibrium studies of Pb2+ ion removal from aqueous solutions by use of nano-silver sol-coated activated carbon. *Braz. J. Chem. Eng.* 339–346.
- Tangboriboon, R.K.N., Sirivat., A., 2012. preparation and properties of calcium oxide from eggshells via calcinations. *J. Mat. Sci.* 30 (34), 313–322.
- Viriya-Empikul, N., Krasae., P., Nualpaeng., W., B.Yoosuk., K Faungnawakij., 2012. Biodiesel production over Ca-based solid catalysts derived from industrial wastes. *J. Fuel.*
- Wang, Heming., Hashimoto., Seiji., Moriguchi., Yuichi., Qiang., Yue Zhongwu Lu., 2012. Lymph node metastasis between sternocleidomastoid and sternohyoid muscle in clinically node-positive papillary thyroid carcinoma. *J. I. Ecol.*
- Woldemedhin, A., A., K., Tekola, B., Mogessie, B., 2021. Evaluation of bentonite clay in modified and unmodified forms to remove flouride from water. *J. Wat. Sci. Technol.*
- Woldetsadik, D., P., D., Keraita., Bernard, Itanna, Fisseha, Gebrekidan., Heluf, 2017. Heavy metal accumulation and health risk assessment in wastewater-irrigated urban vegetable farming sites of Addis Ababa, Ethiopia. *Int. J. Food Contamin.* 4–9. doi:10.1186/s40550-40017-40053-y.
- Wong, KK., L., C., Low, KS., 2003. Removal of Cu and Pb by tartaric acid modified rice husk from aqueous solutions. *Chemosphere* 50 (51), 23–58.
- Yahaya, L.E., A.A., 2016. Equilibrium sorption of Lead(II) in aqueous solution onto EDTA.
- Zahra marghiasi, F.B., Darezereshki, Esmael, Esmaelzadeh, Esmat, 2014. Preparation and characterization of CaO nanoparticles from calcium hydroxide by direct thermal decomposition method. *J. Ind. Eng. Chem.* 113–111.
- Zhang, H., Li-e, Liu., Jindun, Liu., Hongping, Li., Jie, Liu., 2012. Equilibrium, kinetics and thermodynamics studies of Lead (II) biosorption on Sesame husks. *Bio. Resour.* 7 (3), 3555–3572.